SYSTEM TESTS
OF
THE ATLAS SEMICONDUCTOR TRACKER BARREL

By
Björn Skubic

SUBMITTED IN PARTIAL FULFILLMENT OF THE
REQUIREMENTS FOR THE DEGREE OF
MASTER OF SCIENCE
AT
KUNGL. TEKNISKA HÖGSKOLAN
100 44 STOCKHOLM
MAY 2001
TRITA-FYS 9113
ISSN 0280-316x

Contents

Abstract

The ATLAS semiconductor tracker (SCT) is part of the ATLAS inner detector. It will provide space point information on charged particles emerging from the high energy proton-proton collisions produced at the Large Hydron Collider (LHC). The SCT consists of a system of silicon strip detectors that will be read out digitally. Proper grounding and shielding of the SCT is important in order to ensure low noise operation. There are currently two approaches to doing this. An important part of the system test work is to evaluate these two schemes in order to find the one which works best. The system test setup is currently expanding. Preliminary tests have been made on the two grounding schemes on a barrel SCT system with a size equivalent to less than 0.3 % of the actual barrel SCT. No conclusion can been drawn from the system test as to what scheme is most effective, as the system is still too small.

Acknowledgements

I would like to express my sincere gratitude to everybody who has helped me to complete this diploma work and particulary to:

Anders Hugnell at TTA Technotransfer AB for the economic support making my work at CERN possible.

Gunnar Verngren at Mitel Semiconductor AB and Bertil Arvidsson at Ericsson Cables AB for their interest in the project.

Mark Pearce at KTH and Tony Weidberg at Oxford University for arranging my diploma work at CERN.

Jo Pater and Alan Rudge for supervising my work at CERN.

Szymon Gadomski, Pawel Brückman and Martin Morrisey for letting me join them in their work on the barrel system test.

Julio Lozano Bahilo and Alick Macpherson for spending a lot of time introducing me to the system test.

Kristina Gunne at NFR for practical help during my stay.

Björn Skubic
Stockholm
May 4, 2001

Introduction

The ATLAS (A Toroidal LHC ApparatuS) experiment (fig. 1) is one of three experiments being built for studying proton-proton collisions at the LHC (Large Hydron Collider). The detector is designed for studies of a wide range of physics including searches for Higgs bosons, supersymmetric particles, new gauge bosons, leptoquarks, detailed measurements of CP-violation, of the third quark family and measurements on rare B-hadron decays.

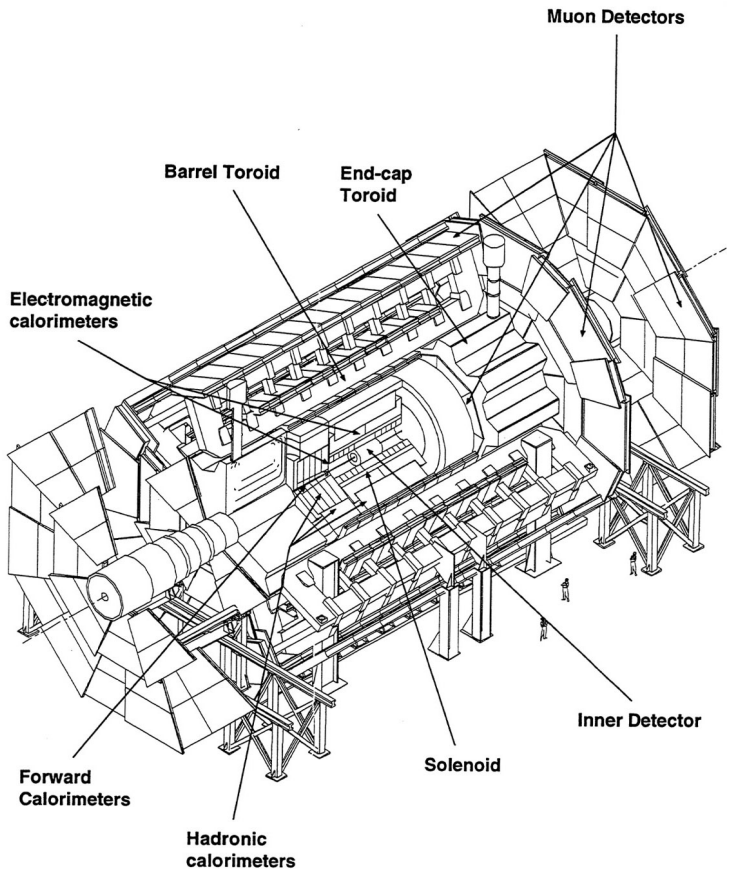

Figure 1: ATLAS

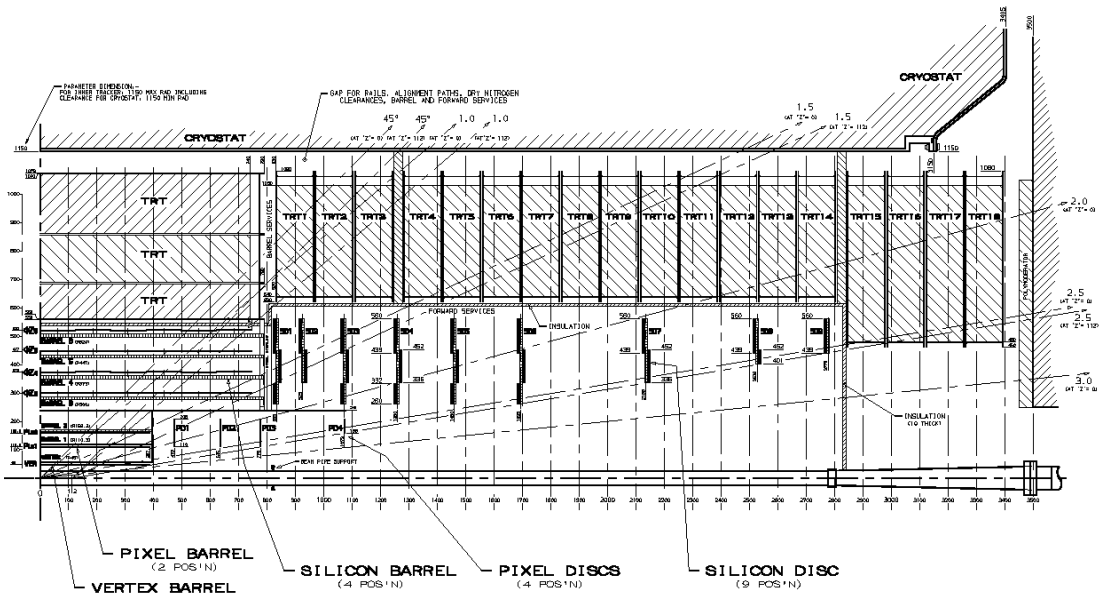

Figure 2: r-z cross section of the inner detector

LHC will carry two counter rotating beams of protons. The protons in each beam will be travelling in bunches separated by 25 ns. At four collision points the two beams are brought together to produce collisions at a bunch crossing frequency of 40 MHz. ATLAS will be placed at one of these crossing points. Approximately 25 proton-proton collisions are expected at each bunch crossing. The ATLAS detector will consist of three basic units that capture information from particles emerging from the collisions. These three units are the inner detector, the calorimeter and the muon spectrometer.

The inner detector (fig. 2) will rest inside the magnetic field of a 2 T solenoid. The purpose of the inner detector is to provide high-precision space points (fig. 3) for tracing the tracks of charged particles emerging from the high energy collisions. The detector will consist of three parts gathering data at different distances from the collision point. The SCT is one of these units. The SCT will consist of 4 barrels and a total of 17 endcap disks covered with silicon strip detectors.

In order to reduce the amount of information read out from the inner detector, a trigger system is used to discard data from collisions that are uninteresting to analyze. The first level (L1) trigger system gathers information from the calorimeter and the muon detector and issues an L1 accept signal if data is to be read out from the inner detector.

The basic readout unit of the SCT is called a module (fig. 4). A module consists of several silicon strip detectors and necessary readout electronics. The SCT will have a total of 4088 modules. There will be three different types of forward modules and one type of barrel module. A barrel module consists of four single sided silicon strip detectors. A barrel detector has an almost square shape (6 cm x 6 cm) and contains a total of 768 readout strips with a pitch of 80 μm. Each detector strip looks electrically like a silicon diode and will be biased by few hundred volts. When a charged high energy particle passes through the strip, a pulse is generated into the front-end circuitry. The result of the chip processing is sent digitally from the module to the data acquisition system as a list of hit channels.

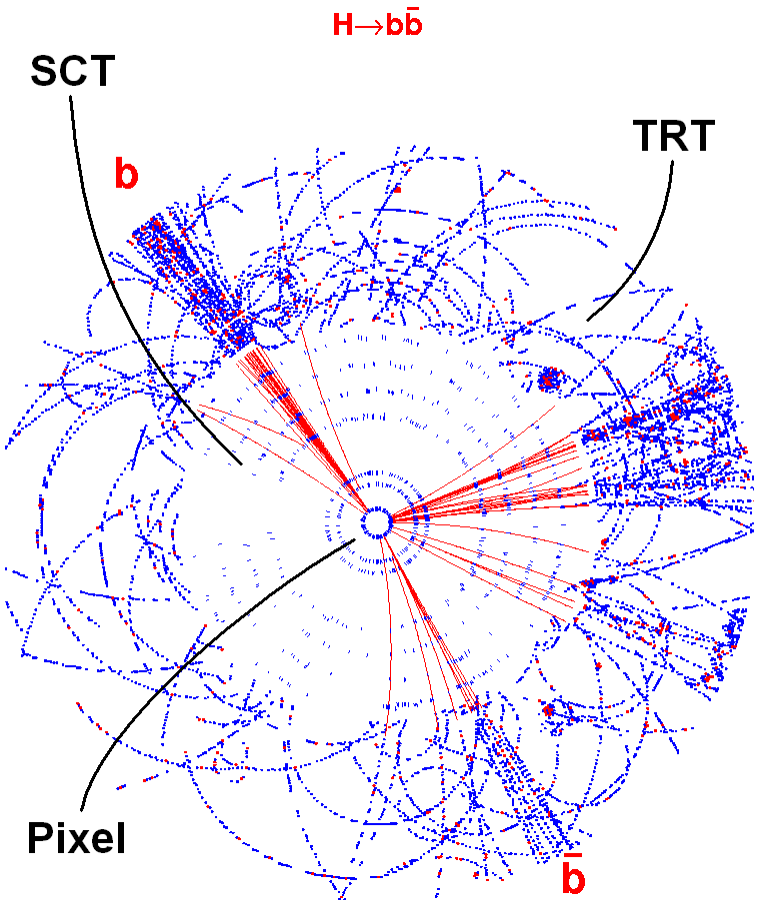

Figure 3: Simulation of an event traced in the ATLAS barrel inner detector. Barrels 4 through 7 belong to the SCT

The grounding and shielding arrangement of the SCT is partially an open question. An arrangement which ensures lowest possible noise operation has to be found. As the design of the SCT is fairly complete, the current grounding and shielding work is focused on testing different schemes within the flexibility of the design. Two different schemes or approaches have been proposed. The main purpose of the system test is to evaluate the different schemes to find a scheme that gives the best performance of the detector.

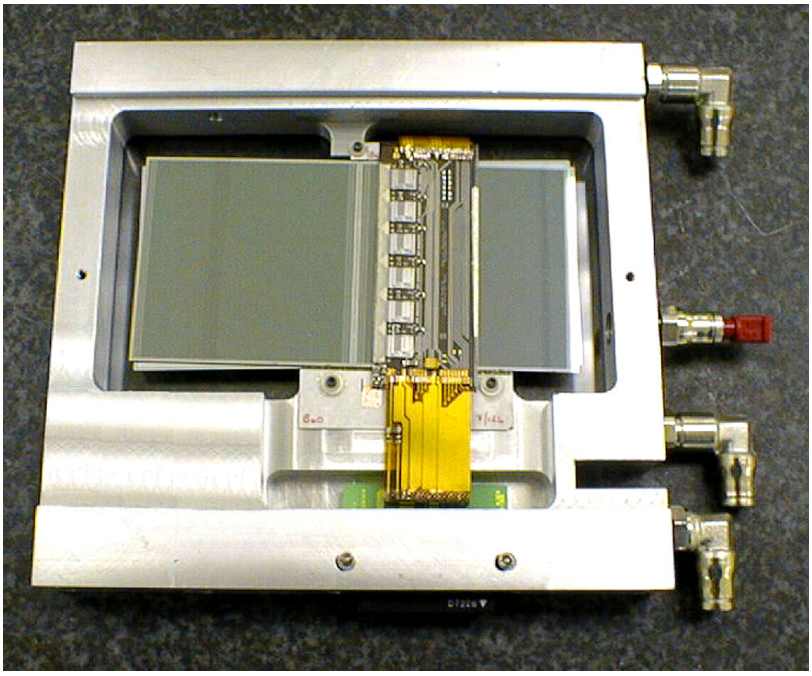

Figure 4: SCT barrel module in a module box. The picture shows the top side of a module with its two top side silicon strip detectors and top side electronics. Each silicon detector is 6 *cm* x 6 *cm*.

Chapter 1

The ATLAS SCT Barrel System

This chapter contains a description of the ATLAS SCT barrel system.

1.1 Introduction

The barrel detector system [5] will consist of four barrels. For each barrel, a cylinder harness of carbon material forms a support structure onto which modules, readout components, cooling pipes etc. are mounted. The baseline solution chosen for the readout of the SCT is a digital optical link. The design must be very reliable incorporating redundancy schemes to minimize data loss. Access for maintenance of the SCT is very limited because of its location deep in ATLAS. The readout system must therefore be able to handle failures such as single chip malfunctions or fibre breaks. Monitor and control possibilities are included in the design so that actions can be taken to prevent damage to the system.

1.2 Module

A barrel module consists of two pairs of daisy chained detectors (fig. 1.1). These pairs are glued onto the front and backside of a thermally conductive base board. The base board sticks out from between the detector at two points of the module. At both these points facing boards are glued to both sides of the base board. The hybrids containing the electronics are fastened to the facings and are not in contact with the silicon detectors. There is a small air gap between the hybrids and the detectors which prevents heat from the chips to reach the silicon. Each of the 12 chips on the module have an average power dissipation of 5.5 W. Low power dissipation is important in order to reduce the risk of thermal run-away of the detector. Low power dissipation also important from a mass reduction perspective since cooling requires mass.

The SCT will run at a environmental temperature of -7 $^{\circ}C$. A temperature cycling between -25 $^{\circ}C$ and 25 $^{\circ}C$ is expected. It is important that the module is capable of elastic deformation, since the temperature of a module can vary a lot between different parts of a module. Locally at some point a module can have a temperature of up to 50 $^{\circ}C$. The precision of the SCT will depend on the module profile after changes in operating conditions.

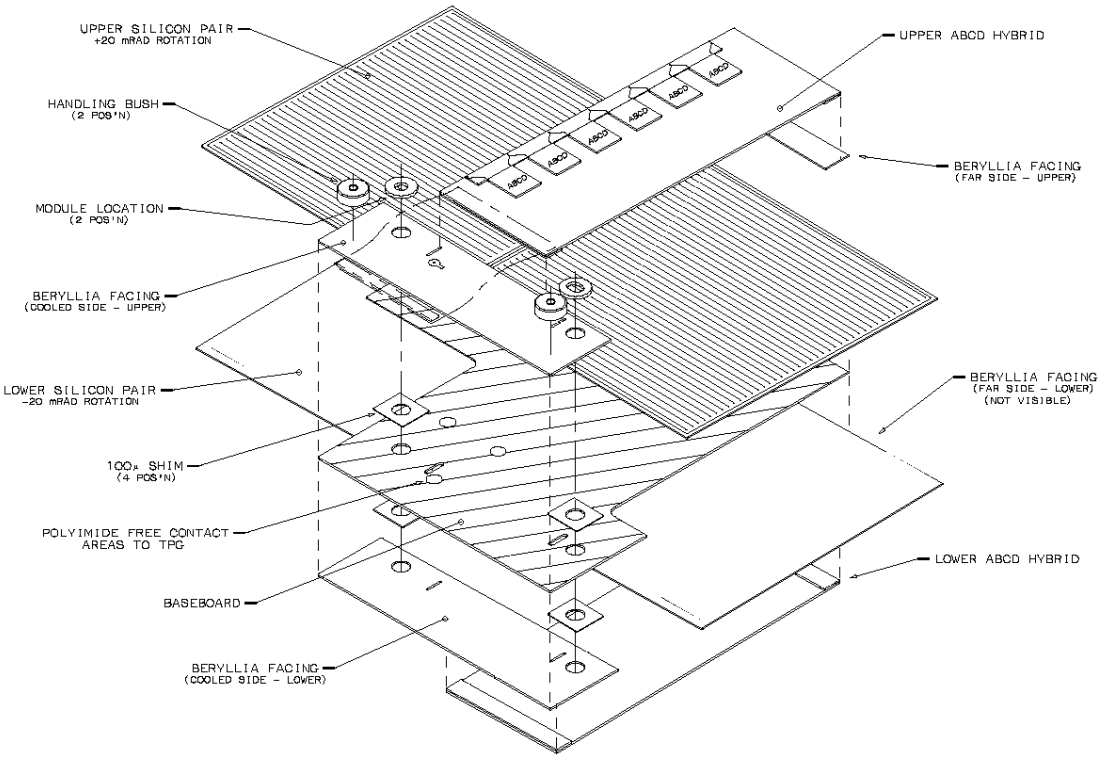

Figure 1.1: SCT Module. Approximate dimensions: 6 cm x 12 cm

1.2.1 Detector

The detector chosen for the SCT is an almost square (63.56 mm x 63.96 mm) p-on n single sided detector [1, 4, 17]. This gives a module strip length of 126.09 mm where there is a dead part of 2,090 mm in the middle where the detectors are joined. Each module has a total of 768 readout strips with a strip pitch of 80 μm. The back side detectors have a strip angle of 40 $mrad$ with respect to the top side detectors. The obtained tracking precision with this system is 17 μm in the r-phi direction and 500 μm in the z-direction. The p-type implant has a width of 18 μm and each p-strip is AC coupled to a 16 μm wide aluminium layer over the p-implant. There are two bonding pads at each end of a strip. A bias ring carries the bias voltage around the strips. The ring is connected to each strip through a bias resistor at one end of the strip.

The SCT will be in an environment of high radiation. The effect of radiation damage on the detectors is an increase in leakage current and a change in effective doping. This reduces the signal to noise ratio and detector efficiency. To keep a high performance of the detector, the bias voltage will be increased as the detector ages. The maximum dose which the SCT is expected to receive during a period of 10 years gives a depletion voltage of 350-400 V.

1.2.2 Front-End Electronics

The front-end electronics consists of an analog stage and a digital stage. The latest front-end chip developed for the SCT module is the ABCD3T [3]. This chip contains both analog and digital circuitry serving 128 of the detector strips.

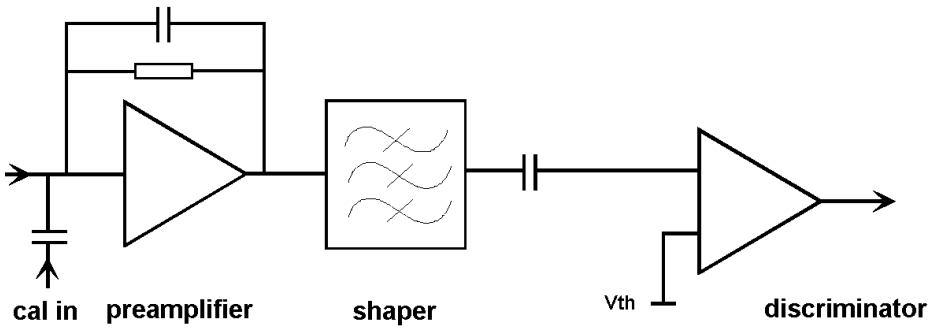

Figure 1.2: Block diagram of analog front end circuit

The analog stage consists of a preamplifier circuit followed by a single gain step, an integrator and a discriminator (fig. 1.2). After passing the amplifying stage the integrator converts the pulse to a voltage level. The voltage level is then compared to the discriminator threshold which is set by the control software. The threshold is set on a chip to chip bases which requires a certain uniformity of the different channels of a chip. In order to achieve this uniformity there is an AC coupling between the shaper and the discriminator to cut off DC offsets. The gain of the amplifying circuit is made high in order to make discriminator offsets negligible.

For each channel there is a 100 fC capacitor at the input of the amplifier. This capacitor is used for test purposes. At a certain control command, a pulse is sent from these capacitors, simulating strip hits. The calibration pulse function is very useful when testing the electronics of the system and was used during all tests in the system test lab.

The digital stage (fig. 1.3) has an input register where data from the discriminator is received in either level or edge sensing mode. At every clock cycle, data is taken from the input register and stored in a 132 bit pipeline for each channel. As an L1 trigger arrives, data from the bunch crossing corresponding to this trigger and the two bunch crossings adjacent to it, is stored in a 24 bit deep readout buffer. Eight events can be stored in this buffer since three bunch crossings are stored for each event. Data is then compressed. The six chips of a side form a link where the first chip is master and the rest form a link of slaves. Data from the chip link is sent to the data acquisition system

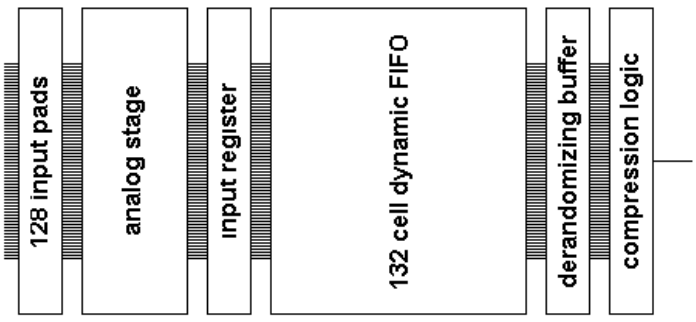

Figure 1.3: Block diagram of ABCD3T chip

through the readout system in a special protocol. The chip link is implemented with a redundancy scheme that can account for single chip failures. If two adjacent chips are bad, data from all chips behind these in the chip link is lost. Another redundancy feature used in case of a master chip failure or a data link failure, is the possibility to read out chips from both sides of a module through one data link.

1.3 Readout System

The readout system for the SCT (fig. 1.4) has several different functions. It is responsible for carrying strip hit information from the silicon strip detectors to the data acquisition system and to the second level trigger. It controls the operation of the SCT, provides bias to the detectors and it provides power to the electronics through a series cables and patch panels (PP3B, PP2B,PP1BW and PP1BN). It also provides means for module calibration and module monitoring. Developing the readout system is a balance between optimizing performance parameters such as noise, detection efficiency, bandwidth and reliability while minimizing power consumption material and cost.

The baseline solution chosen for the readout of the ATLAS SCT is a digital non-return to zero optical link. The advantage of a digital link is that requirements on the optical components are lower than for an analog link. The laser diodes used in the outward link must not be linear as they do in a an analog link. This permits the use of VCSELs which are cheap and radiation hard. Multi-mode optical fibres can be used in a digital link, while an analog link generally requires the use of single mode fibres. Use of multi-mode fibre greatly simplifies the alignment of optical fibres with the VCSELs and PINs.

There are some drawbacks of using a digital readout system [13]. Work has been pursued on an alternative analog readout system. With analog readout, common mode noise is taken care of by simple averaging. There are tricks that can be used in an analog readout system that increase the signal to noise ratio. In a digital readout system a hit is reported when the pulse from a strip exceeds a certain threshold. In an analog system you can look at clusters of strips. Signals from neighboring strips are added and this produces a higher signal to noise ratio. The resolution of an analog readout for a certain pitch between the strips can be increased by using pulse height information in analyzing data. In terms of safety for the detector, analog readout is better since it provides continuous monitoring of the detector.

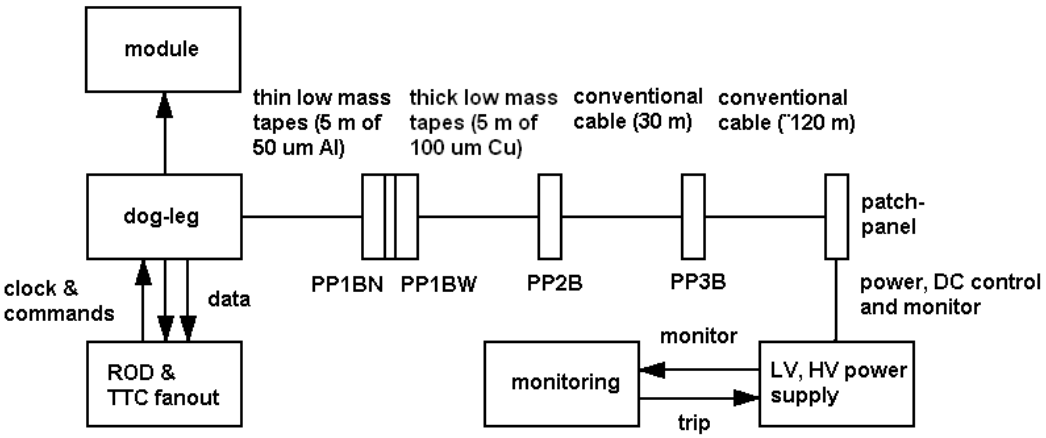

Figure 1.4: Block diagram of the ATLAS SCT system

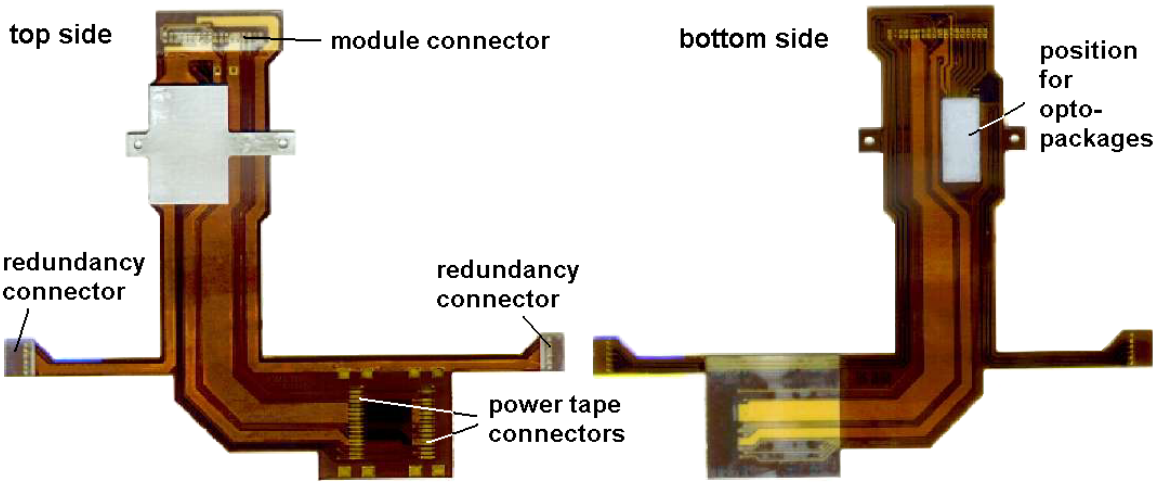

Figure 1.5: Dog-leg

1.3.1 Dog-Leg

The optical packages of the data and control link are separate from the modules. The module interfaces the readout system through an electrical connector.

For each module in the system there is a kapton unit carrying optical packages. This unit which is called the dog-leg (fig. 1.5) is an important part of the system with several different functions. The dog-leg has five electrical connectors, two outward going optical fibres and one inward going optical fibre. One of the connectors connects to the module. Two of the connectors connect to the kapton power tapes that run out to the power supplies. The last two connector are for redundancy purposes and connect to neighboring doglegs.

The purpose of the dog-leg in the system is to constitute the final part of the power supply chain to the module. It makes the conversion of the electrical data output signals to optical signals. It converts the optical input signal containing clock encoded with command (TTC) to an electrical signal. It also contains the DORIC chip which decodes the biphase mark encoding from the TTC signal and extracts the clock and command signal. The kind of malfunction that the redundancy connectors help overcoming is missing clock and command signals to a module. Missing clock and command can occur because of many different reasons such as fibre breaks, power line breaks on the PIN diode voltage, bad PINs or broken bonds on the dogleg. Without redundancy of this kind, such a malfunction would lead to loss of data of a whole module. The redundancy connectors enables a module to use a neighboring modules clock. Commands to a specific module can be bypassed through a neighboring modules control link.

1.3.2 Power Cabling

Four weights of cable are used for supplying power (fig. 1.4). Starting at the power supply unit, there will first be a length of about 120 m of thick conventional cables. These connect to a patch panel PP3B. From PPB3, thin conventional cables will run into to ATLAS to PPB2. From PPB2, the chain continues through 75um thick copper on kapton power tapes to PPB1. From there on 50um aluminium on kapton tapes take over to the dog-legs. Reasons for using fragile kapton tapes instead of conventional cables are for minimizing scattering in the SCT and limiting unnecessary use

of space. Aluminium has four times better conductivity than copper for the same radiation length. This is why aluminium is used for the innermost tapes. Copper will be used for the thicker tapes since low scattering is not that essential in the region of ATLAS where these run. The main problem in this region is space limitation.

The power tapes have individual voltage lines and voltage return lines for the analog and the digital circuitry of the module (fig. 1.6). There is also a special voltage and voltage return line for the high voltage biasing of the module detectors. There are special sense lines for the analog and digital voltages and their returns. These are used for setting voltages more precisely at the modules. The power tapes also carry voltages to the optical packages of the dog-legs (PIN bias, PIN bias return, VCSEL1 voltage and VCSEL2 voltage). There are two lines for reading out the thermistors of the module and two control lines, SELECT and RESET, for more basic settings of the module.

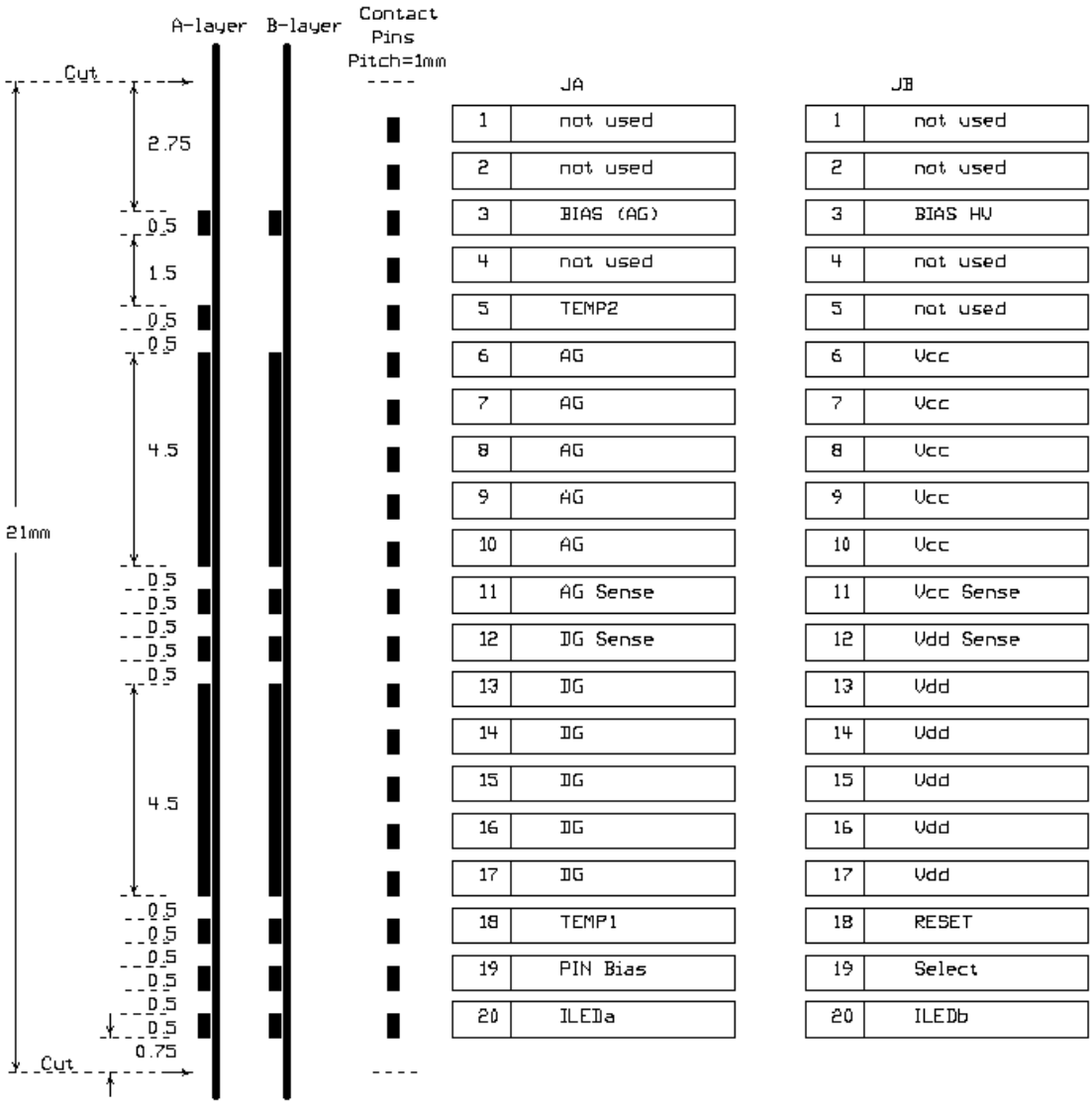

Figure 1.6: Power tape line layout

The patch panels act as an interface between different types of cables. They are also used in different grounding schemes for making necessary connections between different ground lines and implementing choke circuits. The main purpose of the system test is to study different alternatives of grounding and shielding the SCT in order to minimize detector noise. The result of the tests will be used as a contribution to the final design of the SCT. The pieces that are most probable to be influenced by the barrel system test are the patch panels and the electrical connections between different SCT parts such as cooling pipes, thermal shields, module back boards etc. The system test is also a good place to gather experience on other concerns of the system as a whole such as module mounting, power tape reliability, etc.

1.3.3 Opto-Harness

In order to simplify management of the doglegs, the thin low mass power tapes and the optical fibres, these have been connected and bundled together to a unit for six adjacent modules. This is a unit which is called an opto-harness. The input fibres to the six modules are brought together to a 6-way ribbon and the output fibres are brought together to a 12-way ribbon.

1.4 Power Supply

The power supply system provides voltages, logical signals and temperature readout for the SCT modules. There will be one supply per module which means 4088 power supplies. The current design is a switching supply. Advantages of switching power supplies are high efficiency, low heat dissipation, small volume and low price [16]. A problem is the introduction of high frequency noise on the power lines. The power supply is thought to be placed in the service areas remotely from the detector to avoid radiation and magnetic fields levels present close to ATLAS. The maximum cable length expected from the power supplies to the detector is 150 m.

Chapter 2

Grounding Schemes

This chapter will give an overview of the two main approaches of grounding and shielding the ATLAS SCT.

2.1 Introduction

In large experimental setups grounding is a general problem. Ground loops with high currents must be avoided. There are two schemes of grounding and shielding the SCT. Scheme 1, proposed by Ned Spencer [15] at USCS, focuses on eliminating dangerous ground loops. There are ground loops that contain the front-end amplifier of the detector. These loops can lead to strong currents in the small signal path affecting the front-end detector. The basic idea of the grounding and shielding scheme is to shield detectors from each other and create non dangerous paths for noise currents. Scheme 2, proposed by Tony Smith [14] at the University of Liverpool, focuses more on the problem of having voltage differences between different parts of the SCT. To avoid this one should tie all module grounds, shields and cooling pipes together to create an equipotential level in the detector.

2.2 Scheme 1

There is a dangerous ground loop involving pairs of detectors that overlap each other. Because of the detector to detector overlap there is a capacitive stray between module backplanes. These backplanes are capacitively coupled to their respective modules hybrid front end analog ground plane (fig. 2.1). In summary there is an AC coupling between module grounds of different detectors.

Each detector is feed by a separate set of power tapes and power supplies. This causes ground loops in which ground currents can flow (fig. 2.2).

The power tapes of an opto-harness containing tapes for a row of six adjacent module will be brought out of the SCT in bundles. We do not expect great currents in the ground loop of a module pair connected to the same opto-harness. Of greater concern is the ground loop where the power tapes of two adjacent modules are in different tape bundles. Some module pairs will have tapes running out of the SCT in different sides. This could potentially be a big problem.

The way of handling these ground loops in scheme 1 is by placing a shield around the barrel SCT. All the conductors entering the shield are to be shorted or capacitively bypassed to the shield. The idea is to have ground currents running through the shield instead of through the small signal ground (fig. 2.3).

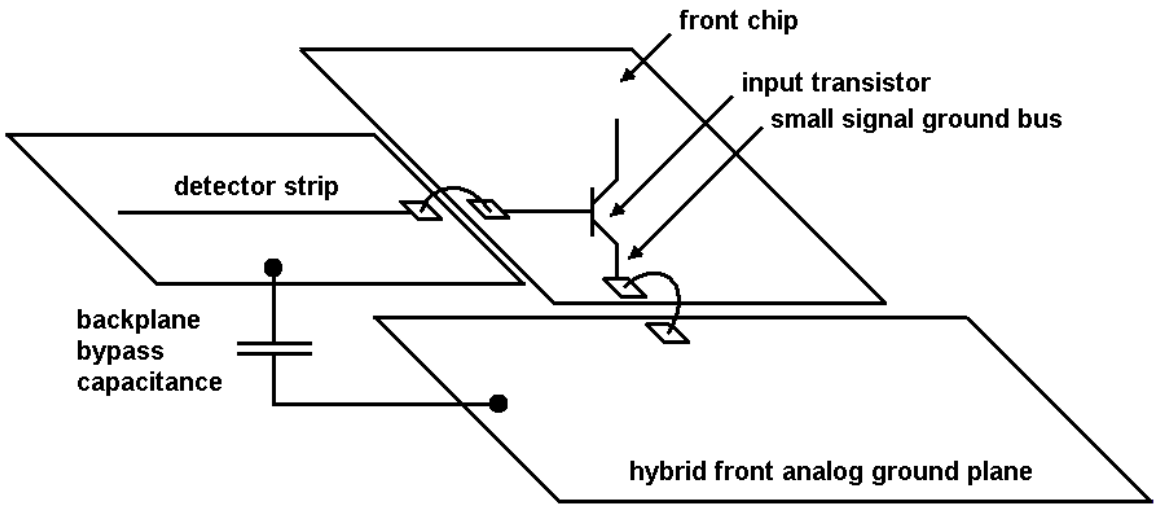

Figure 2.1: Backplane bypass capacitance

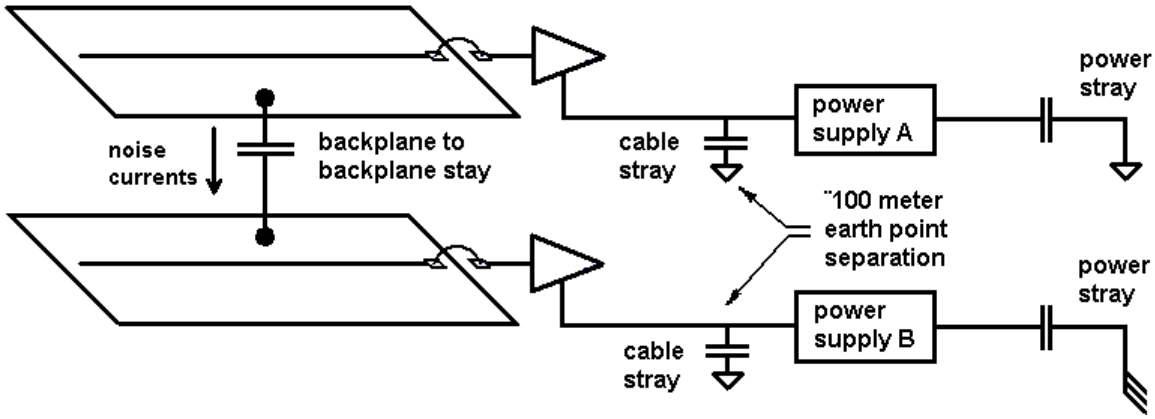

Figure 2.2: Ground loop

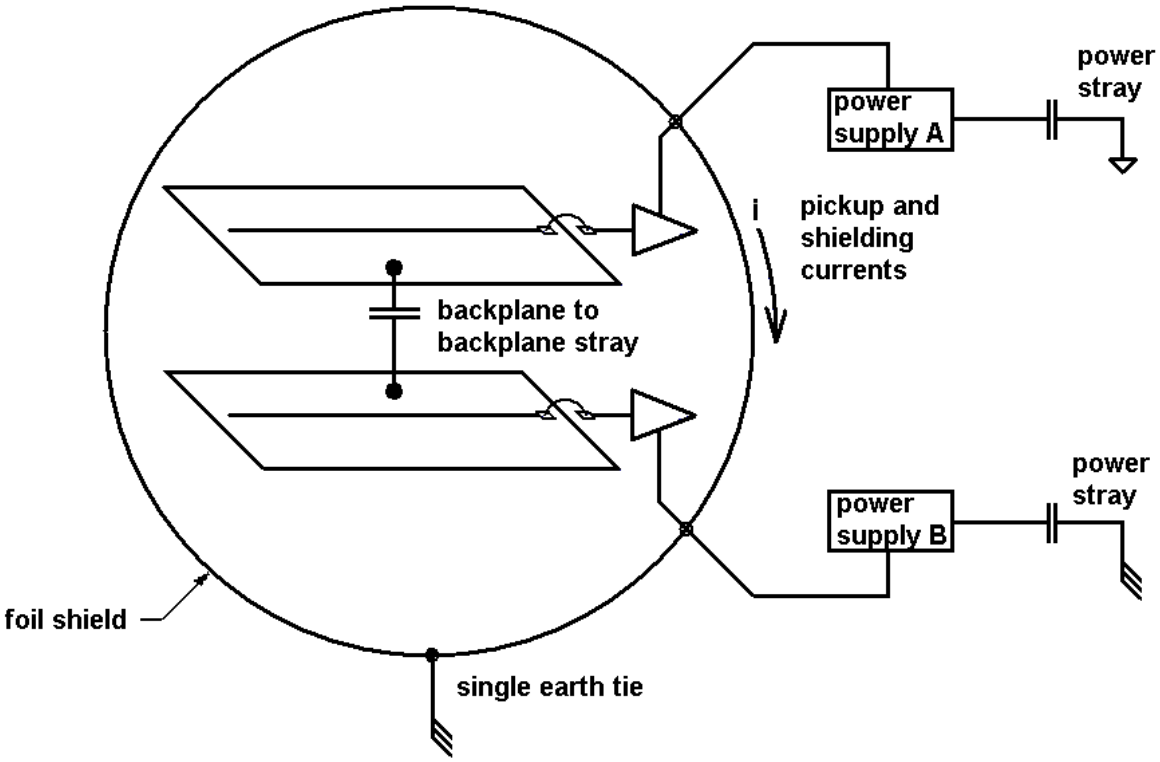

Figure 2.3: New ground loop

In practice this shield is thought to consist of several parts. The idea is to use existing detector parts such as thermal shields and heat spreader plates to constitute the main part. The practical implementation of the shield is therefore complicated.

Cooling tubes will be present and in thermal contact to the modules. The stray capacitance between a cooling pipe and the module can be as large as 100 pF. In addition to ground loops caused by the detector to detector stray capacitance, there will be ground loops caused by the detector backplane to cooling pipe capacitance. The loops caused by this effect might be of worse nature because modules involved can have power cabling taking very different paths into the SCT.

In order to reduce this effect, the cooling pipes will be shorted to the shield at both entry point and exit point if these points are close and only at one point if they are far from each other. The purpose is to minimize the currents in the cooling pipes and have them on the module array shield instead. An important part of scheme 1 is a shunt shield between the detector backplane and the cooling pipe. The shunt shield consists of an extra conductive layer connected to analog ground (AGND) on the dogleg close to the module connector. The idea is to have stray currents flowing through the dog-legs instead of the module backplanes. The shield is meant to reduce the stray capacitance between the module backplane and the cooling pipe to 1 pF.

There is also a proposal in the scheme of connecting AGND of neighboring modules through the redundancy arms of the doglegs. A connection would only be made between modules of the same half of the detector which have power tapes entering at the same end of the barrel.

A plate called the heat spreader plate is chosen as a common for the system. The heat spreader plate and other heat shields will together constitute the barrel module array shield surrounding the

barrel SCT. The parts will be tied together and isolated from external support structures.

Four weights of cable are used for the SCT. There will be the 120 m conventional cables, the 30 m conventional cables, the 5 m of 100 μm thick Cu power tapes and 5 m of 50 μm thick Al power tapes. The conventional cables will have cable shields and the power tape bundles will have a wrap of foil. The wrap of foil starts at the module array shield and ends at PPB2. In general there might be small interruptions of the shield at the patch panels where the different cable weights meet. The shields meeting at PPB2 will be connected. The shields meeting at PPB3 will be connected through a choke. How the shield will be terminated at the power supplies is not specified.

At PPB1 there will be a tie connecting the power tape grounds and the power tape shield to the heat spreader plate. The power tape shield at the end closest to the module will by in ohmic contact to the module array shield. The other end of the foil shield at PPB2 will be in ohmic contact to the heat spreader foot.

2.3 Scheme 2

The other approach to grounding the SCT focuses on the noise voltage between the module array shield and the ground reference point of a module and the noise voltage between the ground reference points of two modules.

The input of the front-end amplifiers of the modules are forced to the same potential as the amplifier ground reference point. If there is a difference in potential between the ground reference point of a module and the surrounding shield, this will appear as a voltage difference between the module silicon face and the shield. A voltage difference between the ground reference points of two modules will appear as a voltage difference between the facing of two modules.

Because of their closeness, there will be some capacitance between the module array shield and the strips of a module. A voltage difference between the shield and a module strip will inject a pulse directly into the front-end amplifier (fig. 2.4). The way of eliminating this risk is to prevent voltage differences from appearing by tying the shield and the hybrid ground plane together.

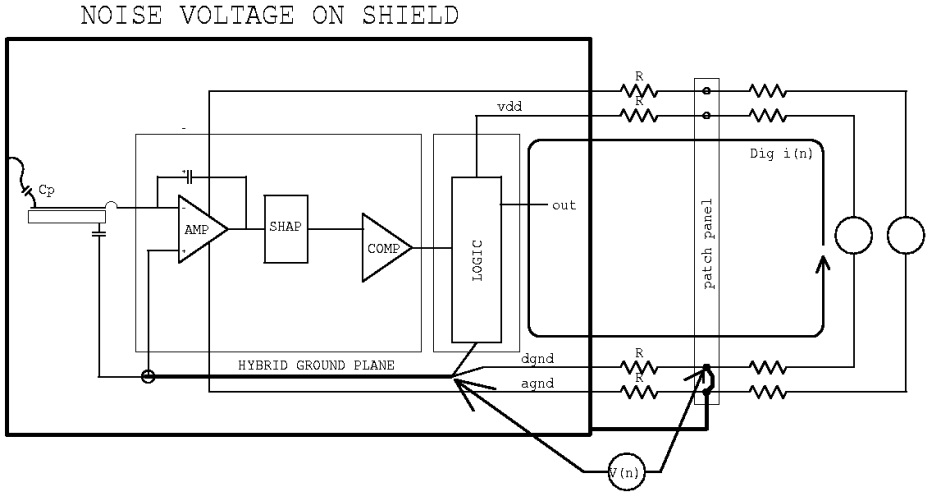

Figure 2.4: Voltage signals generated on shield due to common impedance coupling

Neighboring modules will overlap, giving a capacitance between overlapping strips. If the module facings are of different potentials there will be a pulse injected into the front-end amplifier (fig. 2.5). The problem is solved by shorting the hybrid ground plane of the modules to each other. The proposal is to make this short through the cooling pipes. The scheme gives a common ground plane where hybrids, cooling pipes and shields are tied together (fig. 2.6) as opposed to shielded from each other as in the previous scheme.

The point of each module which should be chosen as the star ground point is the low end of the detector decoupling capacitor. The tie to the cooling tube should be made here. A tie made somewhere else where power supply current exists, introduces a common impedance coupling leading to power supply noise at the amplifier.

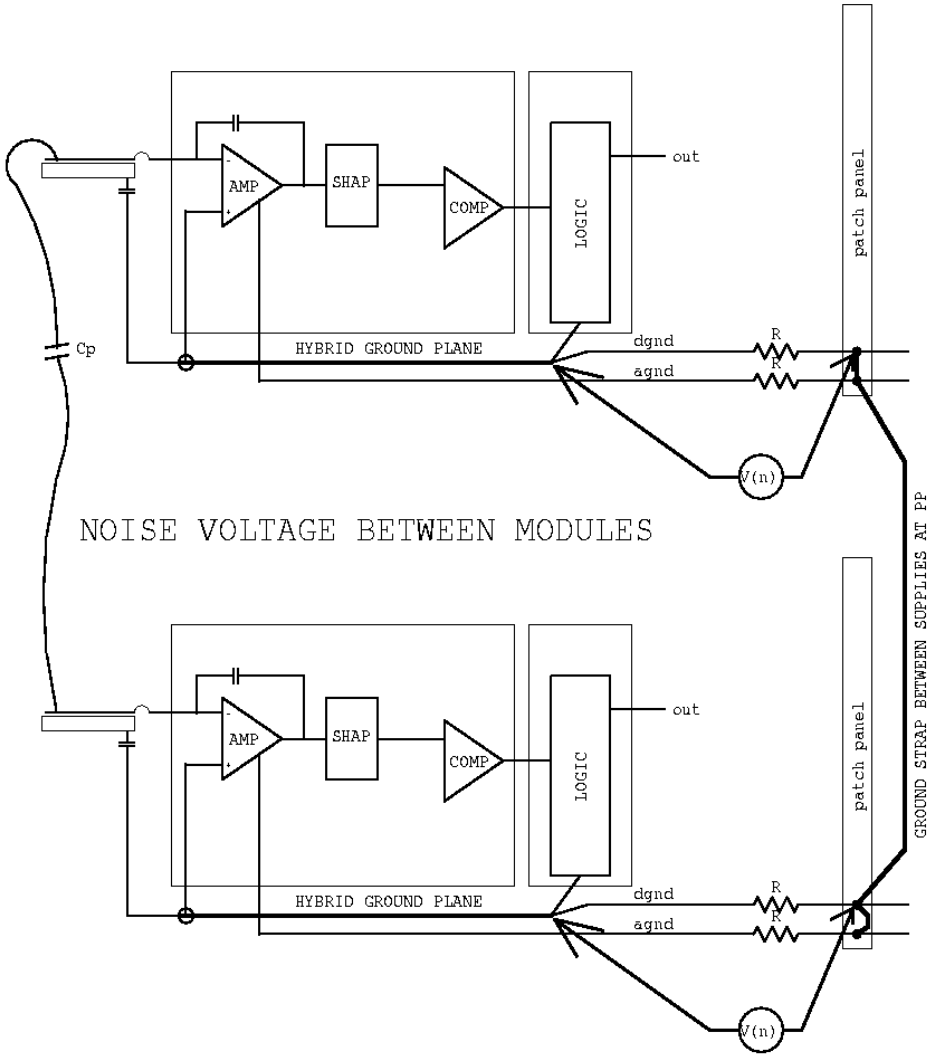

Figure 2.5: Voltage signals generated between modules due to common impedance coupling

It is also important in this scheme that the power supplies are Ohmically isolated at the power supply end. A connection between these would provide a loop for DC noise currents to circulate through.

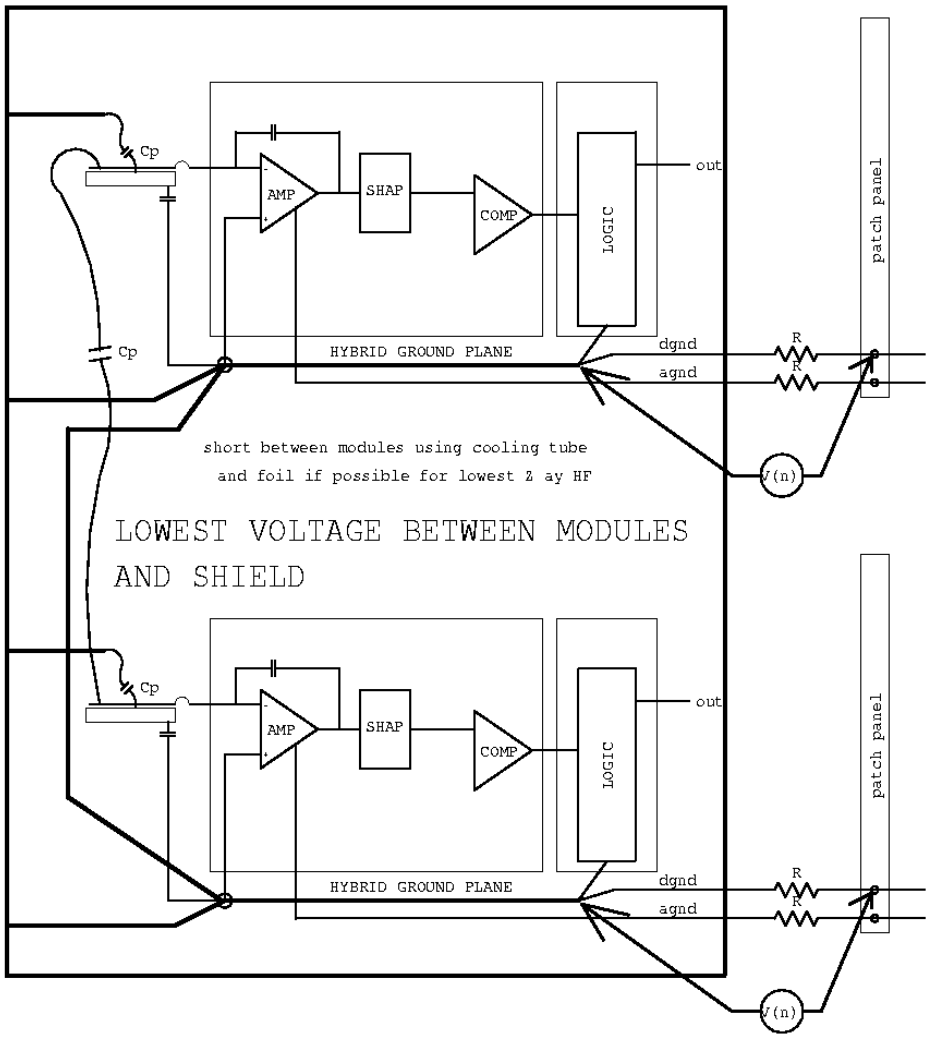

Figure 2.6: The way to eliminate voltage differences

Chapter 3

Methods of Measuring the Performance of a Module

This chapter describes the methods used in the system test for measuring the performance of a module.

3.1 Introduction

The system test is concerned with module performance in different environments. There are several different quantities and plots that are interesting in order to get a picture of the performance of a module. There are also several procedures which can be used for measurements and calculations.

3.2 Noise Measurements

The noise at the input of the discriminator gives a good idea of the performance of a module. Noise measurements at the discriminator stage are made by doing a threshold scan (fig. 3.1(b)). With a specific calibration pulse size you scan through a discrete range of threshold settings of the discriminator. For each threshold a certain number of calibration pulse read outs are made (usually 1000). For a threshold of 0 V all read out attempts record a hit. As the threshold increases, less and less calibration pulses trigger hits. The results can be summarized in an s-curve (fig. 3.1(a)) for each channel showing the number of hits for different thresholds. If no noise was present, the s-curve would look like a step function. An error function is fitted to each channel S-curve. A sigma can be extracted from each curve telling us the noise in mV at the discriminator input for that specific channel.

An equally interesting value for the noise is the noise in e (electrons) right at the input of the analog circuit. This is obtained from the mV noise at the discriminator and the gain in mV/fC of the analog circuitry. The gain of the analog circuitry is measured by doing a series of threshold scans with different calibration charges. The gain is obtained from fitting a curve to the 50% points of the s-curves for the different threshold scans. The slope of this fit at a certain threshold is the gain.

Two macros were used in system test lab for calculating the mV and electron noise. The one which I will refer to as a nobu_scan does threshold scans at the calibration charges 0, 2, and 3 fC. It does a linear fit to calculate the gain and uses the 2 fC threshold scan to calculate the noise values.

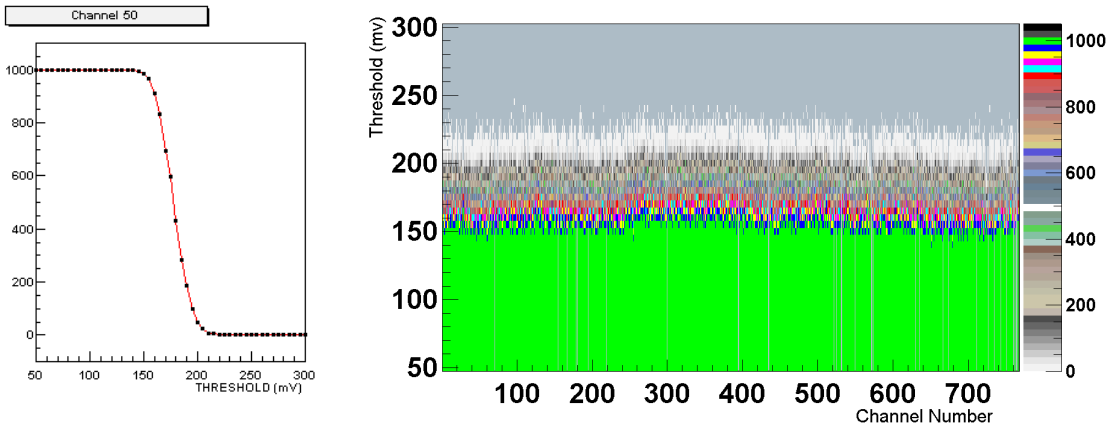

(a) S-curve

(b) Threshold scan

The second macro called stan_kwikgain does threshold scans at 2 fC and 3 fC. It does a linear fit to obtain the gain and calculates the noise at 2.5 fC by using the two threshold scans.

3.3 Stability Measurements

A noise occupancy scan gives an idea of the stability of a module. Here you scan over a discrete threshold range. Instead of specifying the number of readouts for each threshold as in a threshold scan, the number of hits to be read out at each threshold is specified. Readout continues until this number of hits is achieved. For high threshold values data taking is longer than for low threshold values. The occupancy which is the fraction of registered hits is commonly plotted against the discriminator threshold (fig. 3.1). Module instability shows up as a bump in this plot.

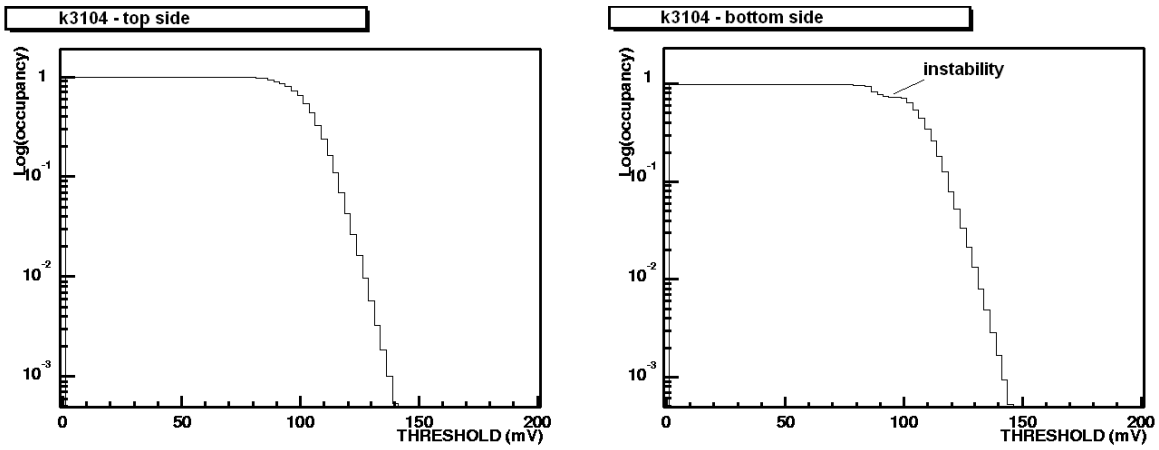

Figure 3.1: Noise occupancy scan

3.4 Common Mode Noise Measurements

Attempts were made to start measuring common mode noise at the barrel system test. Common mode noise can be studied by setting a certain discriminator threshold and making a series of calibration pulse read outs at this threshold. Signs of common mode noise is found by looking at data to see to what extent there are correlations between hits of different strips. There are several different ways of looking at data [9, 12].

The quick way of looking at common mode noise is by making an event by event graph (fig. 3.2). Common mode noise is seen as horizontal lines in this plot. The drawback with this plot is that it doesn't give a value for the noise which can be used for comparisons.

Another way of looking at common mode noise is by pairwise calculating the correlation of channels. The matrix which is produced can be viewed graphically (fig. 3.3). It gives a precise view of the situation but after quite lengthy calculations.

A quick way of looking at common mode noise is by making a histogram of the number of fired channels at each readout (fig. 3.2). The presence of common mode noise is seen as a spread increase of this histogram. Unfortunately the spread also says something of the uniformity of the channel firing percentage for different channels. The spread which can be used for comparing different measurements depends on the common mode noise and on additional factors. Finding good and fast methods of taking and analyzing data is important for the system test future when the number of modules increase.

An issue which has been discussed concerning the common mode noise measurements is at what threshold setting data taking should be done. Running with a threshold giving 50% occupancy has its advantages in giving figures and plots that are easy to interpret. The occupancy in the real experiment will be much lower and there has been a will of doing measurements at the expected SCT occupancy instead. This is very time consuming since it takes a lot of time to gather enough statistics.

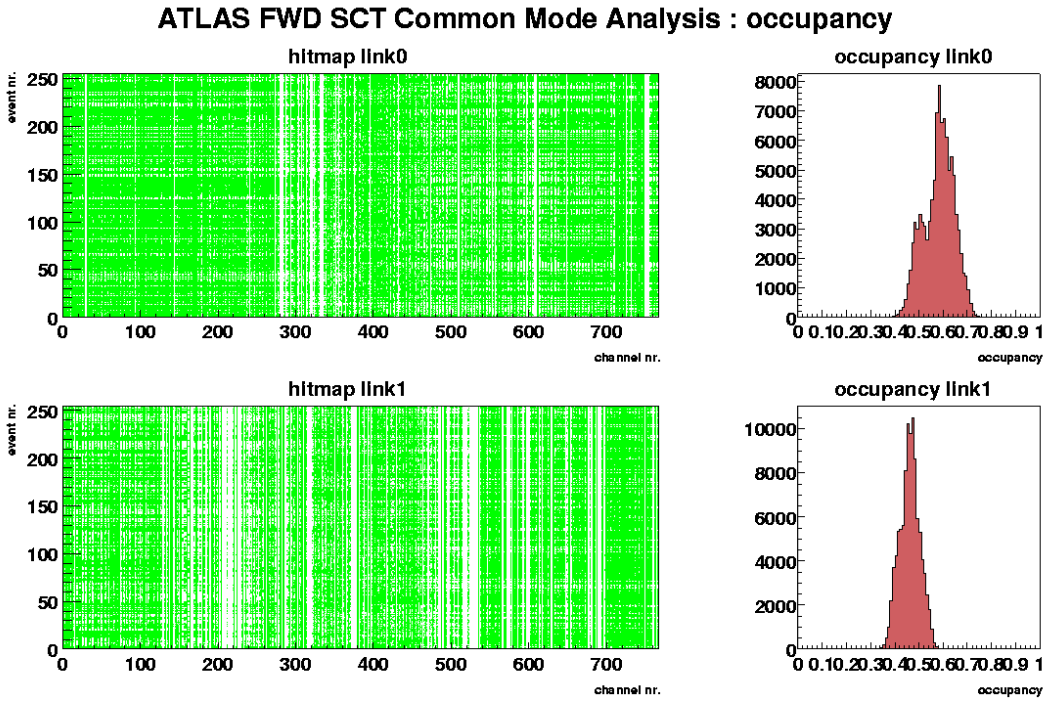

Figure 3.2: Example of event by event graphs and firing histograms

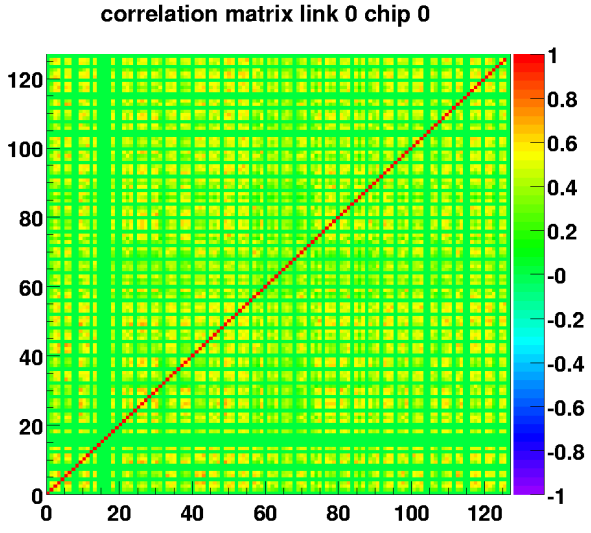

Figure 3.3: Correlation matrix

Chapter 4

System Test of the SCT Barrel

This chapter contains the results of tests done in the barrel system test. Most tests took place during two coordinated system test runs. During the first run three modules were available for the tests and during the second run a total of six barrel modules were available.

4.1 Electrical Stand Measurements

Each module received by the system test lab is characterized off sector in a standard way. The purpose of this off sector characterization is to get performance values that can be used to make comparisons with on sector performance values. The basic idea is to find out how performance changes when modules are placed in system conditions. The plan is to use different grounding schemes to reduce excess noise in the the system setup.

Most modules are tested in off sector conditions at their home institutes. These tests are often done in different conditions, with different module settings and different noise measuring methods. There are several factors that affect the performance of modules off sector. Such factors include the type of module covering, grounding, type of power supply, module settings, type of temperature monitoring, etc. An attempt was made to identify environmental factors that affect noise values. This investigation led to a standard set of conditions for the system test lab. A standard giving as low noise values as possible was chosen. The same environmental factors were then used in testing all modules that came to the system test lab.

4.1.1 Electrical Stand Setup

The electrical stand consists of a Mustard, SLOG, CLOAC system [11] (fig. 4.1). Low voltage supply is provided either through a bench supply or through an SCT-LV2. High voltage is provided through a bench top supply. The electrical stand setup does not have the optical readout link which is used in the system test setup. The module is simply read out electrically. A special support card is used which connects directly to the module box. The electrical stand setup does not use proper cooling. A fan is used for some means of cooling.

Modules are tested in their sealed aluminium box (fig. 4.2) that they come with. Module boxes containing windows are covered with cardboard to prevent light from reaching the modules. Light increases noise values. All tests on the bench and on the system test sector were therefore done with cover.

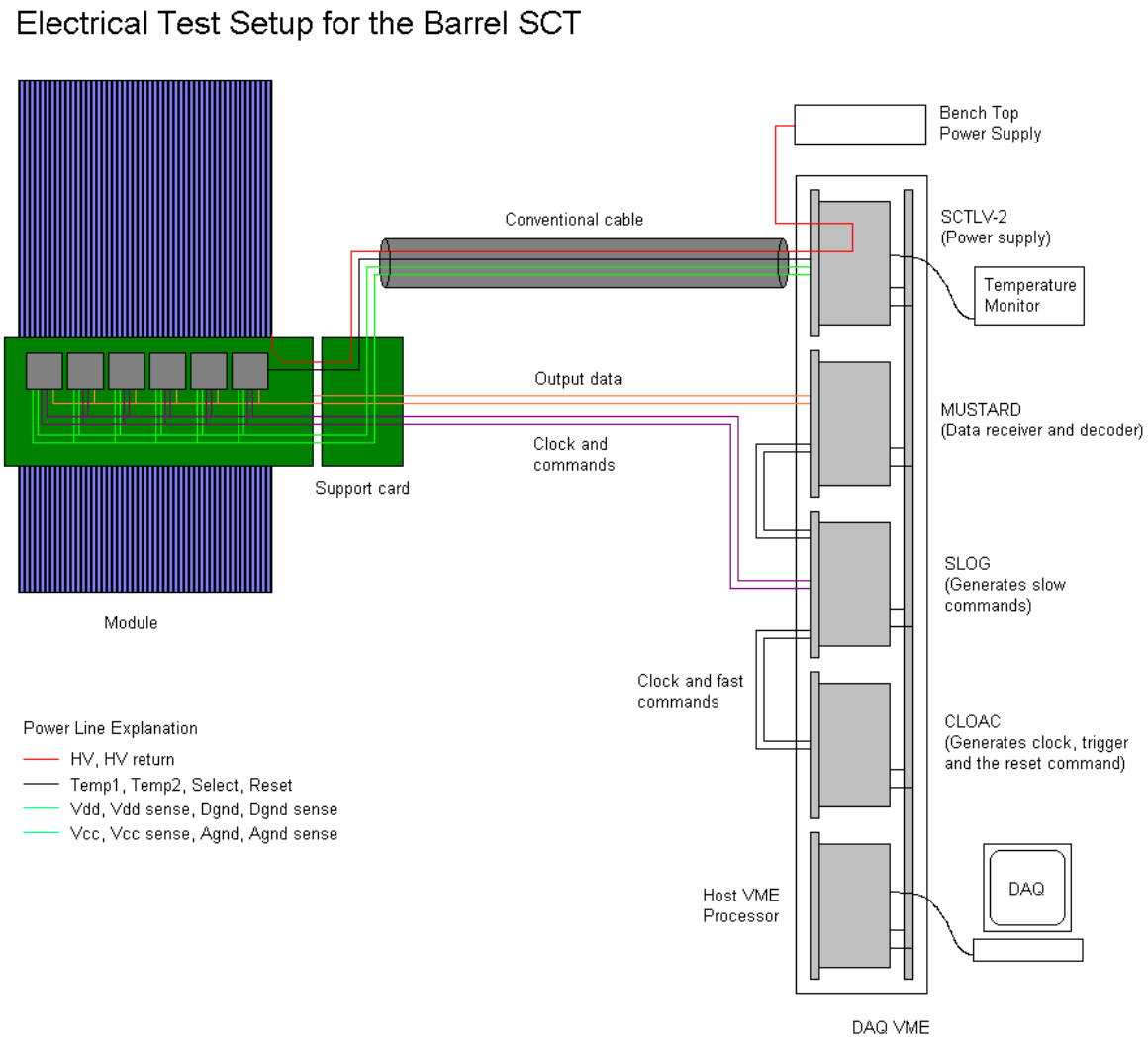

Figure 4.1: Schematic of electrical stand setup

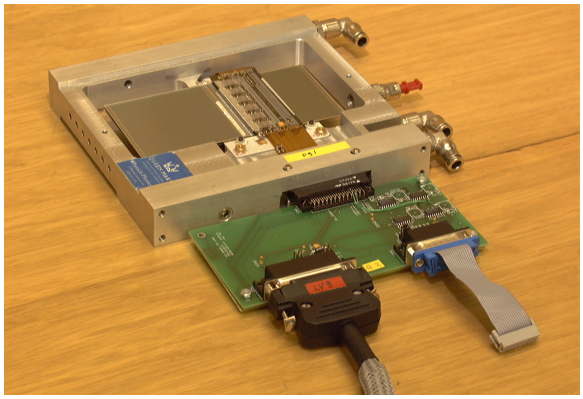

Figure 4.2: Module in module box connected to support card

An investigation was done to see how different ways of providing digital and analog voltages to the modules affect their performance. There showed to be no big difference in results when using the SCT-LV2 together with a choke at PPB2 as of using two bench top supplies. All the standard measurements are therefore done with either two bench top supplies or an SCT-LV2 in combination with a chokes. The SCT-LV2 is a switching power supply which is a prototype for the card to be used in ATLAS. The SCT-LV2 uses sense lines to set the voltages precisely at the module. When using a bench top it is important to measure the voltage at the support card when setting the voltages in order to get the desired voltages at the module.

The value of the detector bias voltage has an effect on the measured noise value (table 4.1). A setting of 150 V was chosen as a standard. This is a value which has been used at KEK (Japan) for their module tests. Using a current meter in the circuit to measure the leakage current seems to have an effect on the noise. We chose not to use a current meter during measurements.

conditions	noise [mV]		noise [e]		gain [mV/fC]	
	top	bottom	top	bottom	top	bottom
100V bias, current meter, no ground strap and temp. monitoring	13.8	13.8	1575	1539	54.7	56.2
standard	12.9	12.9	1465	1431	54.9	56.3
ratio	1.07	1.07	1.08	1.08	1.00	1.00

Table 4.1: Electrical stand performance for k3111 with stan_kwikgain at CERN in under different conditions

The temperature of a module affects its performance. The barrel module has two thermistors which can be read out with a voltmeter. There is an effect on module noise of having a voltmeter connected. Having a voltmeter connected seems to increase noise values. The standard chosen was not to use temperature monitoring in the standard tests. Using a shield on the high voltage line from the bench top supply and tying it to analog ground on the the support card reduces noise. Grounding the module box with a ground strap from the crate ground reduces noise further. These

conditions were chosen as standard. A standard set of module settings were chosen as these also have an effect on measured noise. Level mode was chosen instead of edge and compression mode x1x was chosen for the compression logic. Measurements of all modules were done in these conditions (table 4.2). When fits are made to data you can calculate an error margin which is related to how well data is fit. For all measurements the error in gain is around 1.0-1.5 mV/fC. The error is very seldom above 2.0 mV/fC. Error in mV noise at the discriminator is always in the range 0.20-0.50 mV. The error in electrons is always below 40 e. There are still uncontrolled environmental conditions that influence the results making them difficult to reproduce within an accuracy of 50 e.

Four of the modules that were tested came from KEK. These were tested at KEK and the reported conditions from these tests were: 150 V bias, ground strap from crate to box, bench top supply or SCT-LV2 without choke and cooling box for module cooling.

Noise occupancy scans were done on all modules (fig. 4.3 and 4.4). The bottom sides of k3111 and k3112 show some tendencies to instable behavior at low thresholds. Module rlk6 shows instability on the bottom side.

module	macro	location	noise [mV]		noise [e]		gain [mV/fC]	
			top	bottom	top	bottom	top	bottom
k3103	stan_kwikgain	CERN	12.4	12.6	1604	1648	48.2	47.7
k3103	nobu_scan	CERN	12.7	12.9	1630	1678	48.6	47.9
k3103	nobu_scan	KEK	12.8	12.9	1591	1637	50.4	49.3
k3104	stan_kwikgain	CERN	13.1	13.3	1617	1721	50.7	48.4
k3104	nobu_scan	CERN	13.2	13.4	1678	1755	49.2	47.7
k3104	nobu_scan	KEK	12.5	12.3	1551	1587	50.2	48.5
k3111	stan_kwikgain	CERN	12.8	12.8	1384	1380	57.7	57.8
k3111	nobu_scan	CERN	12.9	12.9	1465	1431	54.9	56.3
k3111	nobu_scan	KEK	12.2	12.2	1437	1409	53.1	54.0
k3112	stan_kwikgain	CERN	12.6	12.8	1343	1362	58.8	58.9
k3112	nobu_scan	CERN	12.7	12.9	1445	1423	54.9	56.7
k3112	nobu_scan	KEK	12.6	12.9	1442	1441	54.8	56.1
rlk6	stan_kwikgain	CERN	13.3	13.1	1420	1400	58.4	58.7
rlk6	nobu_scan	CERN	13.4	13.4	1538	1534	54.3	54.8
scand1	stan_kwikgain	CERN	13.7	12.9	1703	1620	50.4	49.9
scand1	nobu_scan	CERN	13.5	13.0	1738	1668	48.6	49.0

Table 4.2: Electrical stand performance of different modules

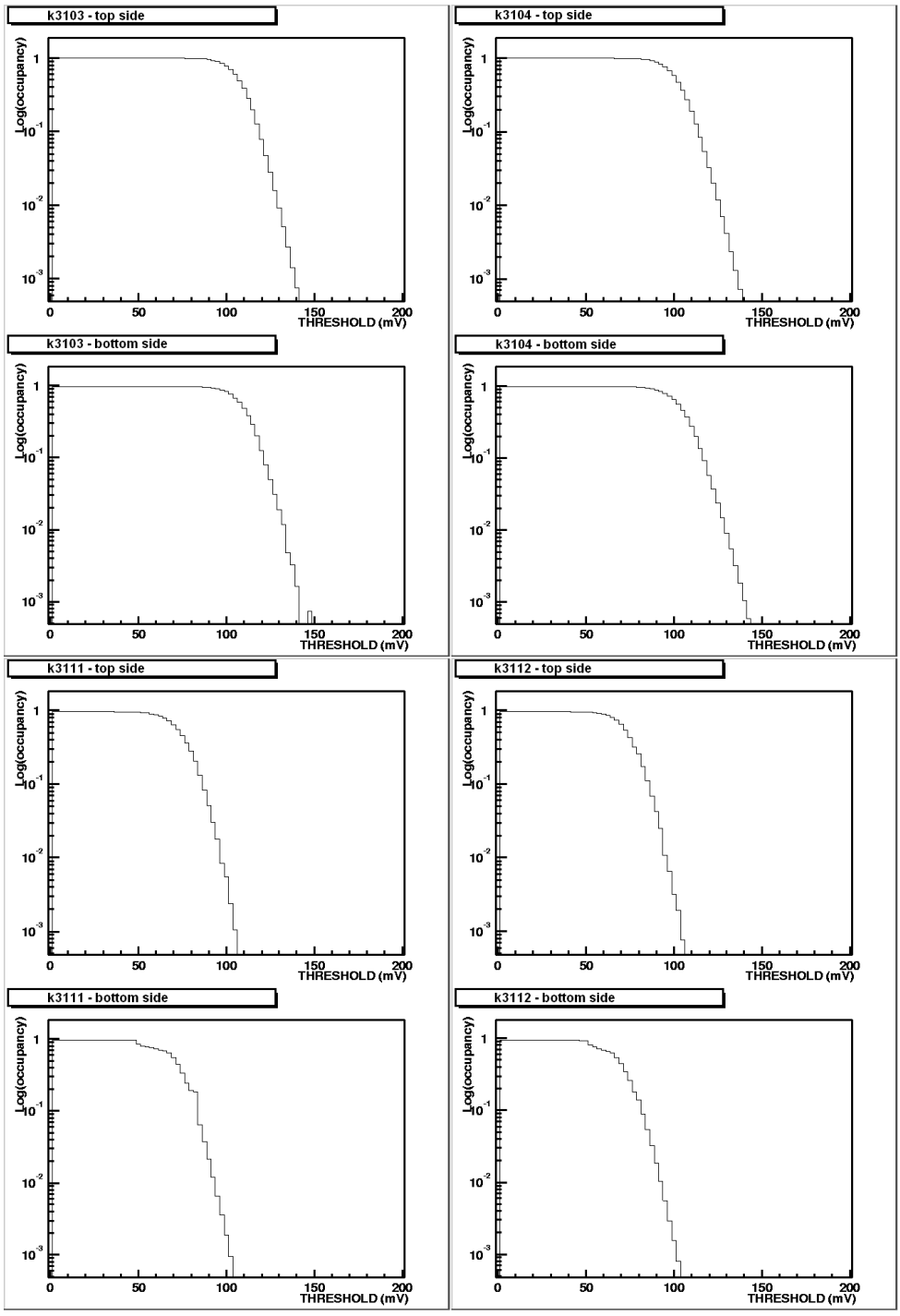

Figure 4.3: Noise occupancy scans for modules on the electrical stand

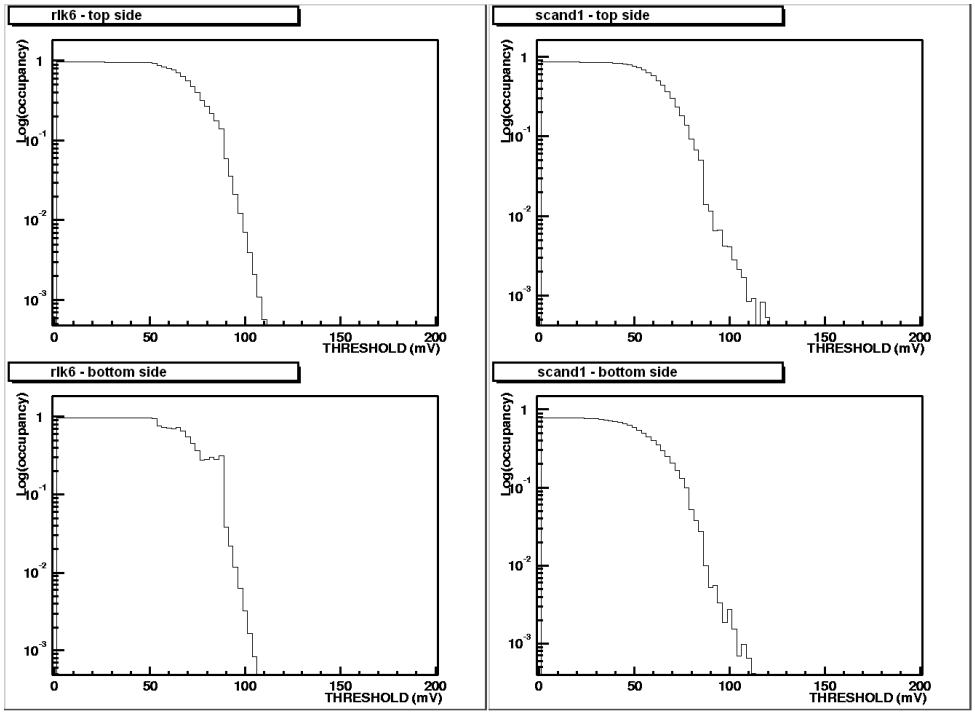

Figure 4.4: cont. noise occupancy scans for modules on the electrical stand

4.2 System Test

The system test setup (fig. 4.5) has evolved during the period of time that the tests were made. Several design changes have taken place and will take place. The dog-legs, power tapes and patch panels used in the tests were of several different versions. The two cooling pipes used on the system test sector have a flat profile. The pipe design for the final SCT will change to a thicker pipe with a round profile.

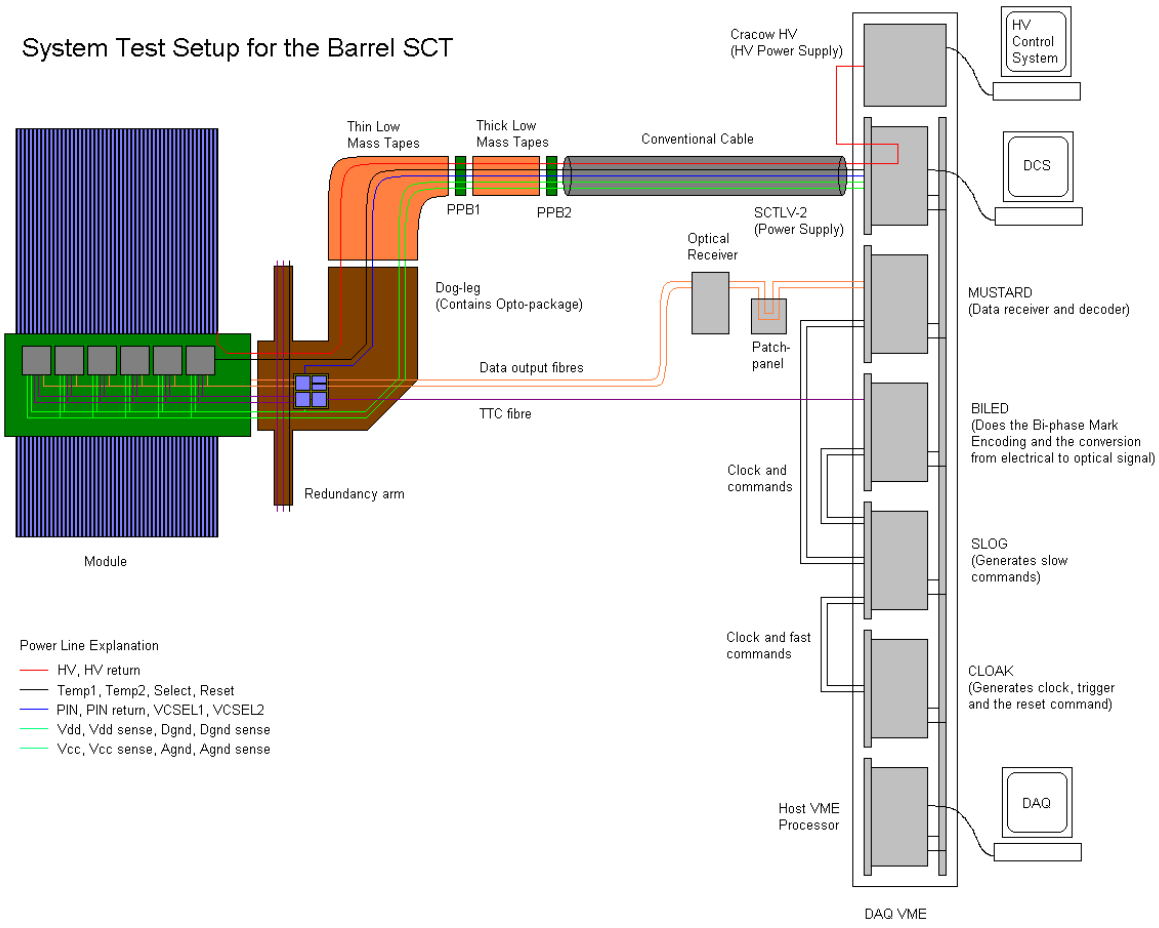

Figure 4.5: System test setup

4.2.1 System Test Setup

The base of the system test setup is a piece of the SCT carbon cylinder structure (fig. 4.7). The structure has the full length of the real SCT cylinder with room for twelve modules in a row. The radius of this cylinder piece is approximately the radius of the smallest barrel. Three rows of modules can be mounted on the piece. This limits the system which can be tested to a number of 36 modules.

Because of other limitations to the setup, tests yet done on December 2000 were all done on just one of the three rows (fig. 4.6), while preparation for using a second row was in full progress.

The sector has a lid which is mounted as a cover when taking measurements. This lid prevents modules from being exposed to light and seals the sector from the surrounding. Humidity under the lid is reduced with dry nitrogen flush.

The setup consists of a Mustard, SLOG, CLOAC system [11]. Low voltage power is provided by the SCT-LV2. High voltage power supply is provided through a special high voltage unit. A Biled board provides the conversion of electrical TTC signals to optical TTC signals which are sent to the dog-legs. A CERN built optical receiver is used for converting optical data signals from the opto-harness to electrical signals which can be interpreted by the Mustard.

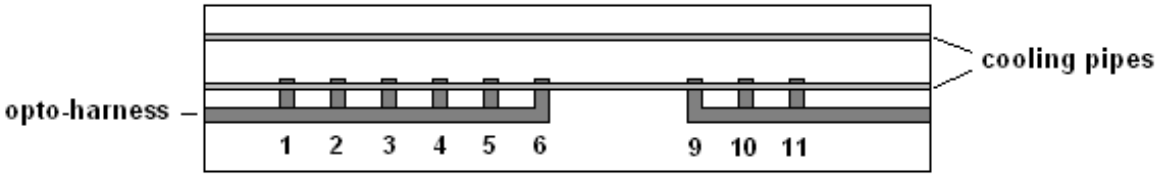

Figure 4.6: Schematic of system test sector piece with nine doglegs. Positions 3,4,5,9,10 and 11 were used in the tests

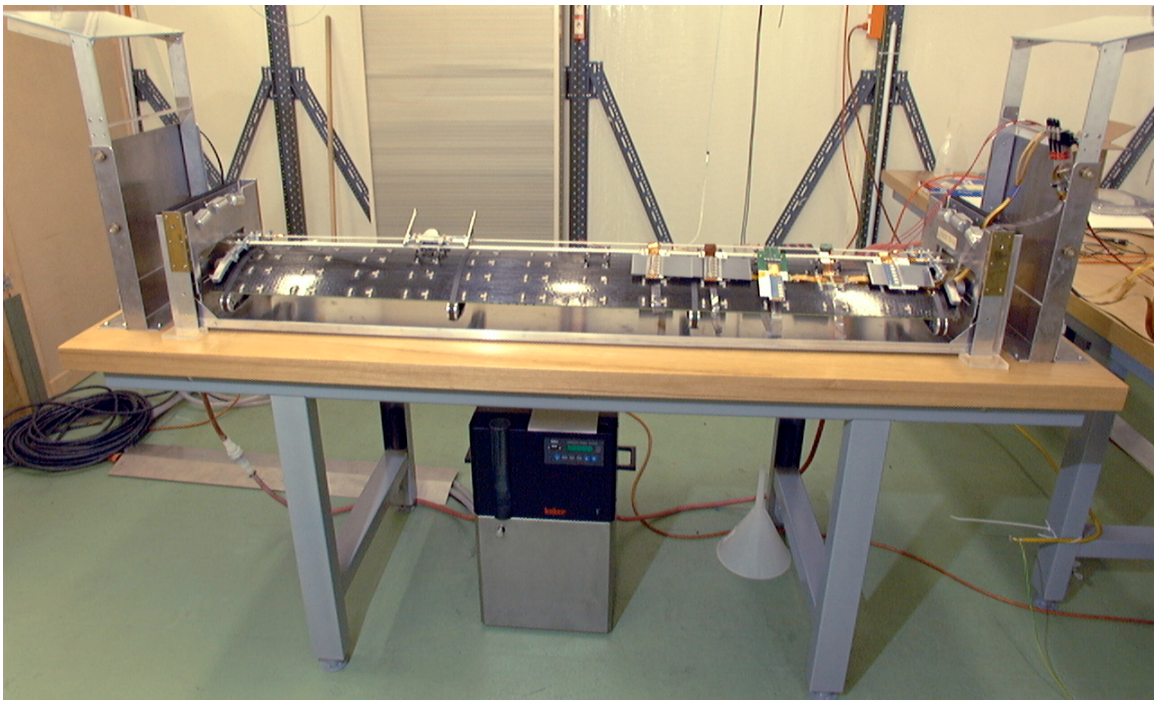

Figure 4.7: Bare system test sector piece

4.2.2 Scheme 2

An attempt was made to implement grounding scheme 2. One important part of this scheme is the DC tie between the cooling pipe and the front analog ground plane. The cooling pipe could not be tied to the decoupling capacitor on the module. A tie was instead made between the pipe and an analog ground pad on the dog-leg. The tie was made with a thin wire (fig. 4.8), which does not really give the scheme justice. The reason for this implementation was to avoid too much tampering with the module. Another important part of the scheme is the DC tie between grounds of different modules and the shield. The system test sector shield consists of the aluminium sector lid and foil wrap around the power tapes. The DC ground tie was made by soldering thin wires from the thin power tapes to the foil shield.

The module performance values in this configuration are quite consistent with the results from the electrical stand (table 4.3). We are not seeing much excess noise for any of the modules on the system test sector. There is therefore no reason for trying to improve the implementation of the grounding scheme.

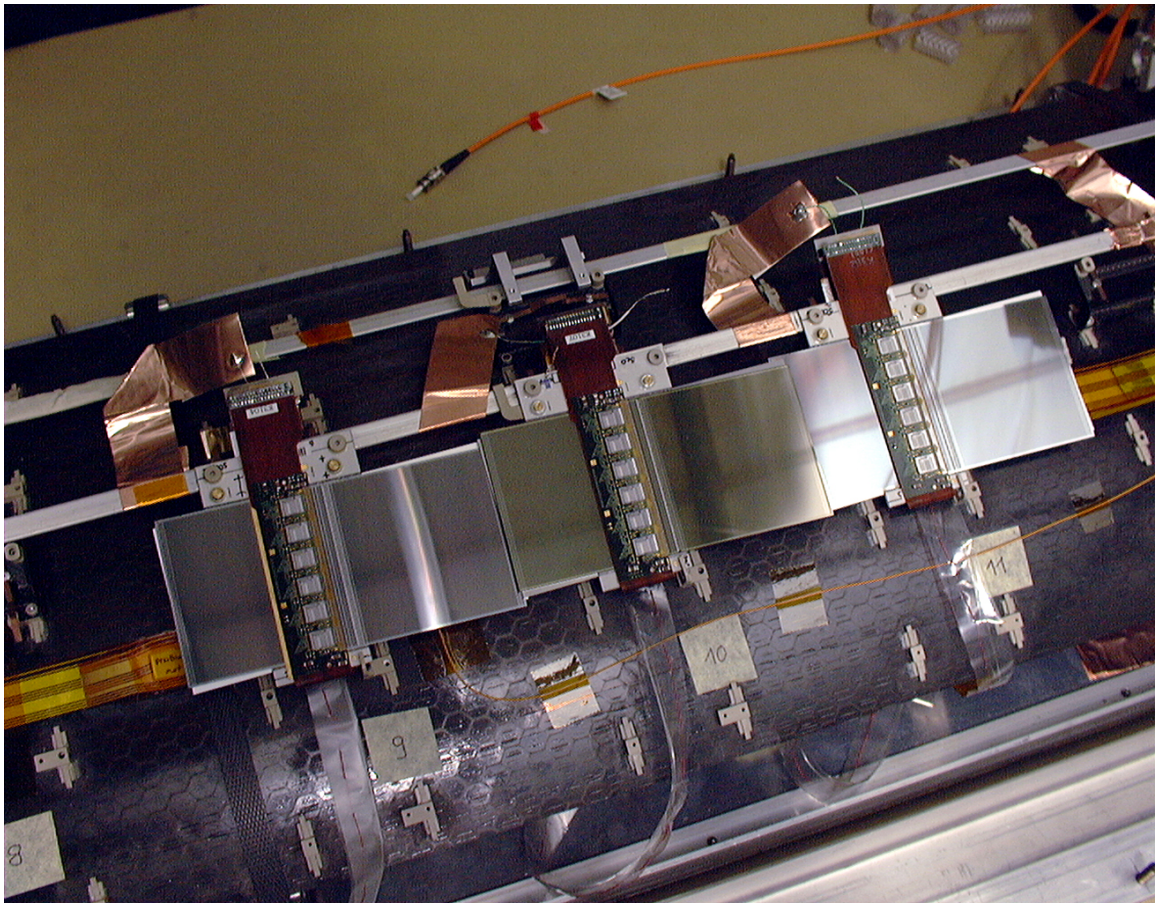

Figure 4.8: Modules k3104, scand1 and k3112 tested on the sector with a DC connection between AGND and cooling pipe.

4.2.3 Scheme 1

Important features of scheme 1 are the shunt shield between module and cooling pipe, AC or DC connection of ground lines to the sector shield at PPB1 and the single tie between cooling pipe and sector shield. The shunt shield was implemented by placing a thin piece of 'copper on kapton' on the cooling pipe where the module and cooling pipe are in contact. The copper layer was connected to the analog ground pad of the dog-leg. Some thermal grease was placed between the kapton and the the cooling pipe. A higher module temperature results in worse performance of the module. It is therefore important to keep the thermal contact between pipe and module as good as possible. PP1B has been prepared for AC connection of ground lines to the sector shield. The connection is removed by removing jumpers. Implementing a DC connection here is more difficult why measurements were made with the AC connection. It is very difficult to draw any conclusions from the results of these measurements (table 4.4). Noise values differ slightly from the ones measured on the electrical stand but they differ in both directions.

4.2.4 Five Module Test

A strive of the system test is to run as many modules as possible at the same time. A five module run was done. Three adjacent modules were placed on one sector half in a DC grounding scheme. The other two modules were placed one module space apart from each other on the other sector half. It was not possible to implement a complete grounding scheme on this sector half at this time. The purpose of the test was to get an idea of the effect of adding more modules to the system. The results are compared to the electrical stand measurements (table 4.5). For module k3111 we see an increase in noise of 4-10 % depending on what values we look at. This module was one of the two that were missing a sensible grounding scheme. One of the modules, scand1, has surprisingly better performance on sector than off sector. The noise values of the three remaining modules are close to the ones measured on the electrical stand.

Noise occupancy scans were done on all modules (fig. 4.2.6 and 4.2.6). The bottom sides of modules k3104, k3111 and k3112 show slight features of instability at low thresholds. The step on the top side of module k3112 at high threshold is due to a problem in the readout software.

4.2.5 Redundancy Scheme

Tests were done on a module using the redundancy link to drive it. As reference the same module configuration was read out without using the redundancy link. No significant difference in noise was observed (table 4.6). More interesting than the noise values is probably the fact that the redundancy readout which had not been tried before worked.

4.2.6 Chokes

Several tests have been done to see what effect chokes have on the noise in different system configurations. Earlier tests done in the system test using an earlier power supply prototype card SCT-LV1, report significant differences in values of noise in measurements with and without chokes. Similar differences, although very small, were observed on the electrical stand. Two sets of measurements were done with somewhat differing environmental conditions and a small increase in noise is seen on all modules when chokes are removed (tables 4.7 and 4.8).

measurement	nobu_scan				stan_kwikgain			
	noise [mV]		noise [e]		noise [mV]		noise [e]	
	top	bottom	top	bottom	top	bottom	top	bottom
k3104(9)	13.3	13.3	1654	1685	13.1	13.0	1572	1649
k3104(elec.)	13.2	13.4	1678	1755	13.1	13.3	1617	1721
ratio	1.01	0.99	0.99	0.96	1.00	0.98	0.97	0.96
scand1(10)	13.2	12.7	1675	1595	13.0	12.6	1579	1531
scand1(elec.)	13.5	13.0	1738	1668	13.7	12.9	1703	1620
ratio	0.98	0.98	0.94	0.96	0.95	0.98	0.93	0.95
k3112(11)	12.8	13.0	1434	1413	12.7	13.0	1308	1341
k3112(elec.)	12.7	12.9	1445	1423	12.6	12.8	1343	1362
ratio	1.01	1.01	0.99	0.99	1.01	1.02	0.97	0.98

Table 4.3: Modules k3104, scand1 and k3112 tested on positions 9, 10 and 11 in grounding scheme 1. General conditions: DC connection to cooling pipe, DC connection between grounds at PPB1, chokes inserted at PPB2

measurement	nobu_scan				stan_kwikgain			
	noise [mV]		noise [e]		noise [mV]		noise [e]	
	top	bottom	top	bottom	top	bottom	top	bottom
k3112(3)	13.3	13.6	1486	1463	13.2	13.5	1342	1368
k3112(elec.)	12.7	12.9	1445	1423	12.6	12.8	1343	1362
ratio	1.05	1.05	1.03	1.03	1.05	1.05	1.00	1.00
k3104(4)	14.2	14.4	1756	1811	14.0	13.9	1635	1728
k3104(elec.)	13.2	13.4	1678	1755	13.1	13.3	1617	1721
ratio	1.08	1.07	1.05	1.03	1.07	1.05	1.01	1.00
scand1(5)	13.6	13.0	1692	1605	13.4	12.8	1571	1494
scand1(elec.)	13.5	13.0	1738	1668	13.7	12.9	1703	1620
ratio	1.01	1.00	0.97	0.96	0.98	0.99	0.92	0.92

Table 4.4: Modules k3112, k3104 and scand1 on positions 3, 4 and 5 in grounding scheme 1. General conditions: AC connection to cooling pipe, AC connection between grounds at PPB1, chokes inserted at PPB2

measurement	nobu_scan				stan_kwikgain			
	noise [mV]		noise [e]		noise [mV]		noise [e]	
	top	bottom	top	bottom	top	bottom	top	bottom
k3111(3)	14.0	14.2	1583	1541	13.9	14.1	1442	1450
k3111(elec.)	12.9	12.9	1465	1431	12.8	12.8	1384	1380
ratio	1.09	1.10	1.08	1.08	1.09	1.10	1.04	1.05
k3103(5)	13.3	13.0	1672	1655	13.1	12.8	1614	1612
k3103(elec.)	12.7	12.9	1630	1678	12.4	12.6	1604	1648
ratio	1.05	1.01	1.03	0.99	1.06	1.02	1.01	0.98
k3104(9)	13.6	13.8	1696	1747	13.5	13.4	1609	1698
k3104(elec.)	13.2	13.4	1678	1755	13.1	13.3	1617	1721
ratio	1.03	1.03	1.01	1.00	1.03	1.01	1.00	0.99
scand1(10)	13.2	12.7	1680	1590	13.2	12.7	1610	1541
scand1(elec.)	13.5	13.0	1738	1668	13.7	12.9	1703	1620
ratio	0.98	0.98	0.97	0.95	0.96	0.98	0.95	0.95
k3112(11)	12.9	13.2	1441	1451	12.7	13.1	1312	1346
k3112(elec.)	12.7	12.9	1445	1423	12.6	12.8	1343	1362
ratio	1.02	1.02	1.00	1.02	1.01	1.02	0.98	0.99

Table 4.5: Modules k3111 and k3103 tested on positions 3 and 5 without specific grounding scheme. General conditions: No shunt shield, no DC connection to cooling pipe, no connection of ground lines to sector shield, chokes inserted at PPB2. Modules k3104, scand1 and k3112 tested on positions 9, 10 and 11 in grounding scheme 1. General conditions: DC connection to cooling pipe, DC connection between grounds at PPB1, chokes inserted at PPB2.

measurement	nobu_scan				stan_kwikgain			
	noise [mV]		noise [e]		noise [mV]		noise [e]	
	top	bottom	top	bottom	top	bottom	top	bottom
redundancy	14.0	14.2	1729	1786	14.0	13.8	1624	1707
reference	13.7	13.9	1700	1751	13.6	13.6	1593	1687
ratio	1.02	1.02	1.02	1.02	1.03	1.01	1.02	1.01

Table 4.6: Module k3104 on sector position 4, receiving TTC through redundancy link from position 3. General conditions: AC connection between module and cooling pipe, AC connection between grounds at PPB1, wrap from shield to PPB1, chokes inserted at PPB2.

measurement	nobu_scan				stan_kwikgain			
	noise [mV]		noise [e]		noise [mV]		noise [e]	
	top	bottom	top	bottom	top	bottom	top	bottom
k3104(9), no chokes	13.4	13.4	1664	1702	13.2	13.1	1584	1670
k3104(9), chokes	13.3	13.3	1654	1685	13.1	13.1	1572	1649
ratio	1.01	1.01	1.01	1.01	1.01	1.00	1.00	1.01
scand1(10), no chokes	13.4	12.9	1693	1620	13.2	12.8	1608	1566
scand1(10), chokes	13.2	12.7	1675	1595	13.0	12.6	1579	1531
ratio	1.02	1.02	1.01	1.02	1.00	1.02	1.02	1.02
k3112(11), no chokes	12.9	13.3	1444	1439	12.9	13.2	1321	1359
k3112(11), chokes	12.8	13.0	1434	1413	12.7	13.0	1308	1341
ratio	1.01	1.02	1.01	1.02	1.02	1.02	1.01	1.01

Table 4.7: Modules k3112, scand1 and k3104 on sector positions 9, 10 and 11 respectively. General conditions: DC connection between module and cooling pipe, DC connection between grounds at PPB1, wrap from shield to PPB1, chokes are inserted at PPB2 when used.

measurement	nobu_scan				stan_kwikgain			
	noise [mV]		noise [e]		noise [mV]		noise [e]	
	top	bottom	top	bottom	top	bottom	top	bottom
k3112(3), no chokes	13.1	13.9	1467	1490	13.0	13.3	1312	1354
k3112(3), chokes	13.0	13.3	1454	1433	12.9	13.3	1313	1351
ratio	1.01	1.05	1.01	1.04	1.01	1.00	1.00	1.00
k3104(4), no chokes	14.1	14.2	1748	1800	13.8	13.8	1630	1726
k3104(4), chokes	13.9	14.0	1727	1768	13.8	13.6	1618	1694
ratio	1.01	1.01	1.01	1.02	1.00	1.01	1.01	1.02
scand1(5), no chokes	13.7	13.3	1708	1645	13.6	13.1	1581	1526
scand1(5), chokes	13.7	13.1	1708	1626	13.5	12.9	1580	1512
ratio	1.00	1.02	1.00	1.01	1.01	1.02	1.00	1.01

Table 4.8: Modules k3112, k3104 and scand1 on sector positions 3, 4 and 5 respectively. General conditions: AC connection between module and cooling pipe, AC connection between grounds at PPB1, wrap from shield to PPB1, chokes are inserted at PPB2 when used.

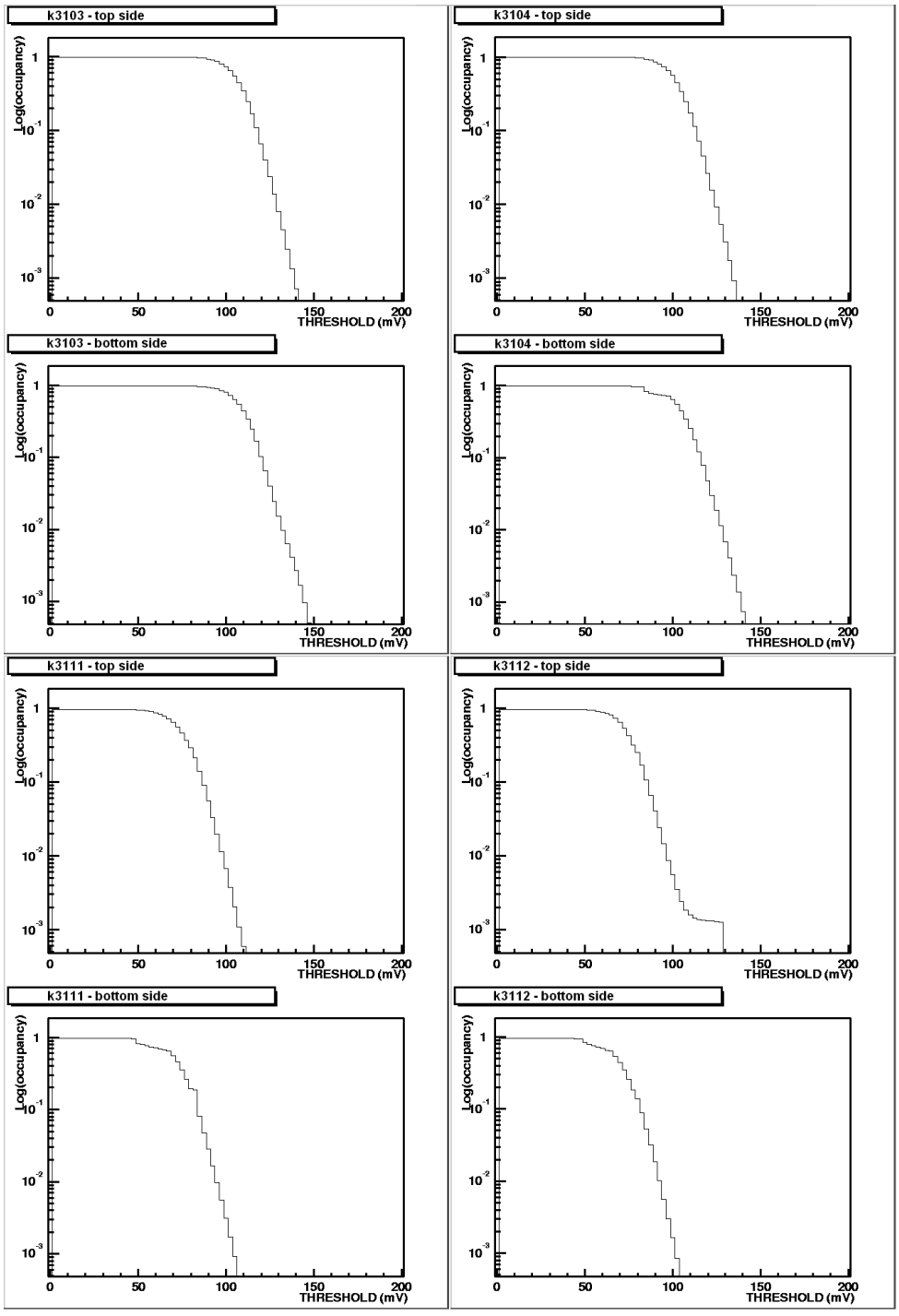

Figure 4.9: Noise occupancy scans for modules in the five module run

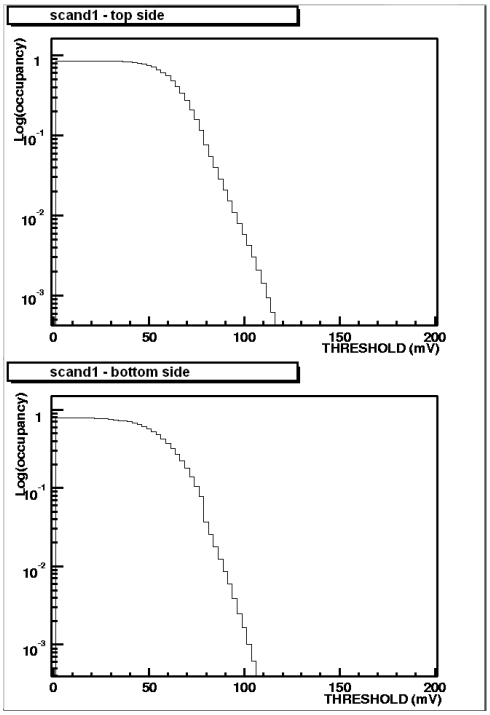

Figure 4.10: cont. noise occupancy scans for modules in the five module run

4.3 Measurements while Injecting Noise

The effect of putting modules on the sector did not result in a great increase in noise. An increase in noise is expected as the system gets sufficiently large. In order to be able to draw conclusions on how to ground the system, measurements have been done injecting noise artificially. This is not very easy since it is very difficult to do this in a way which resembles the way noise is introduced in the real system. The system is complicated and it is very difficult to keep control over what is actually injected. Any vast conclusions cannot be drawn from these measurements, but in absence of a larger system they might give some interesting preliminary results.

4.3.1 Injecting Noise on Cooling Pipes

Work has been done on injecting noise onto the cooling pipe [7]. The focus of these measurements was on evaluating the effect of the shunt shield rather than a whole grounding scheme. Three adjacent modules were used in the test (fig. 4.11). A shunt shield was implemented for all of these. Measurements were done for the shunt shield scheme and the DC connection scheme. The shunt shield setup was easily converted to the DC scheme by bypassing the shunt shield with some copper tape. The cooling pipe was terminated by a 50 Ω resistor. Sinusoidal signals of 2-32 MHz were injected. The sensitivity of the ABCD chip is greatest around 10 MHz and this is also where the signal causes most interference for both schemes. The module performance was slightly better when using DC connection rather than using the shunt shield (fig. 4.12 and 4.13). An interesting observation is that there is quite a significant chip dependance, where the chips on the bottom side of the modules are more affected than the chips on the top side. Common mode noise was measured both with and without the parasitic signal on the cooling pipe. As seen in the event by event graphs (fig. 4.14 and 4.15) common mode noise is increased greatly by a signal on the cooling pipe.

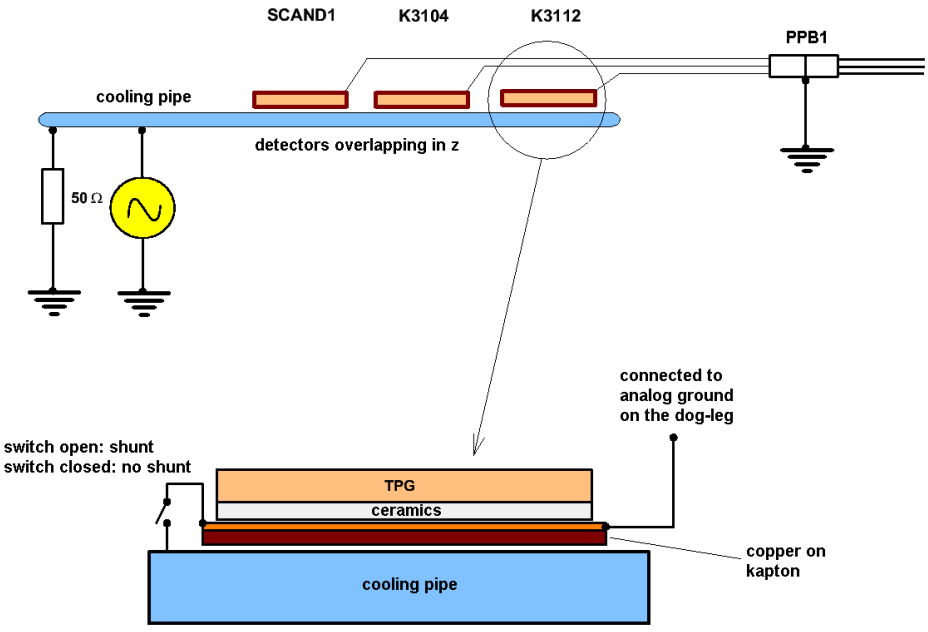

Figure 4.11: Setup for injecting noise on cooling pipe

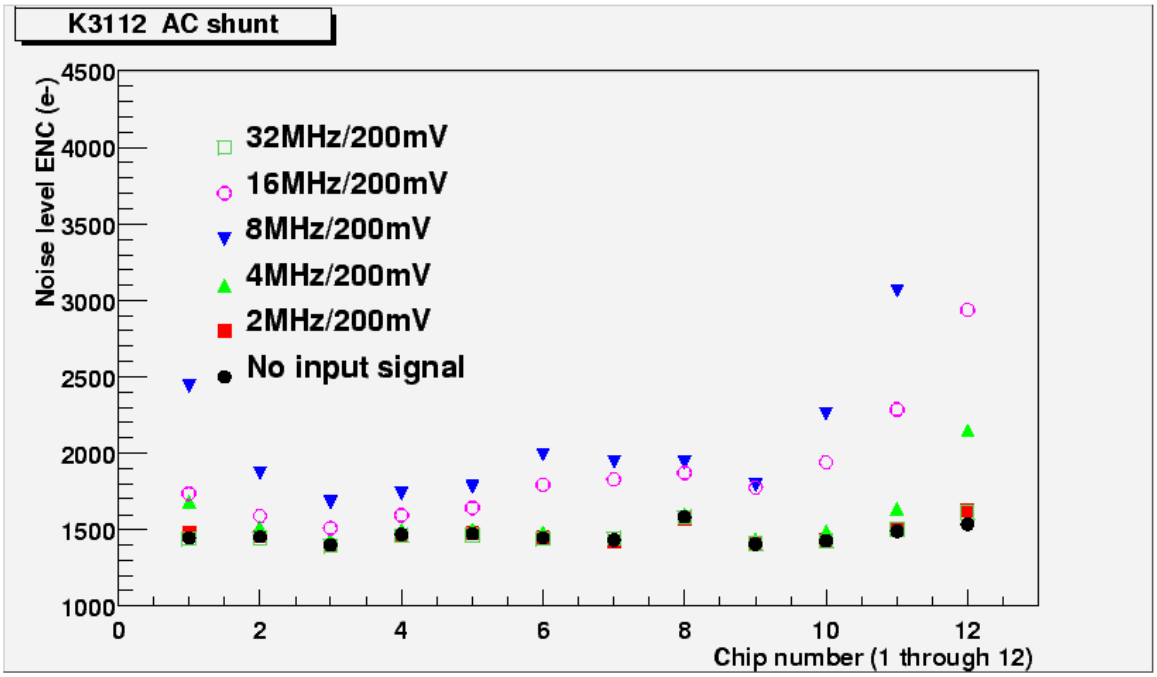

Figure 4.12: Module k3112 with parasitic signal on cooling pipe. There is an AC shunt between module and cooling pipe.

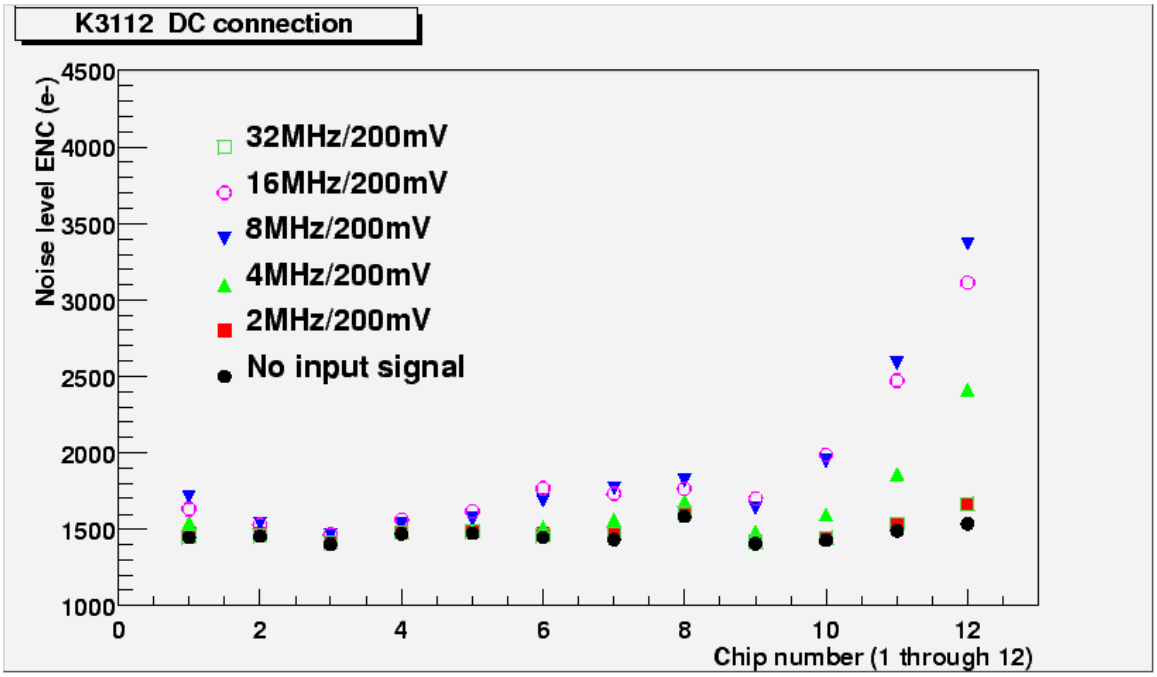

Figure 4.13: Module k3112 with parasitic signal on cooling pipe. There is an DC connection between AGND on dog-leg and cooling pipe.

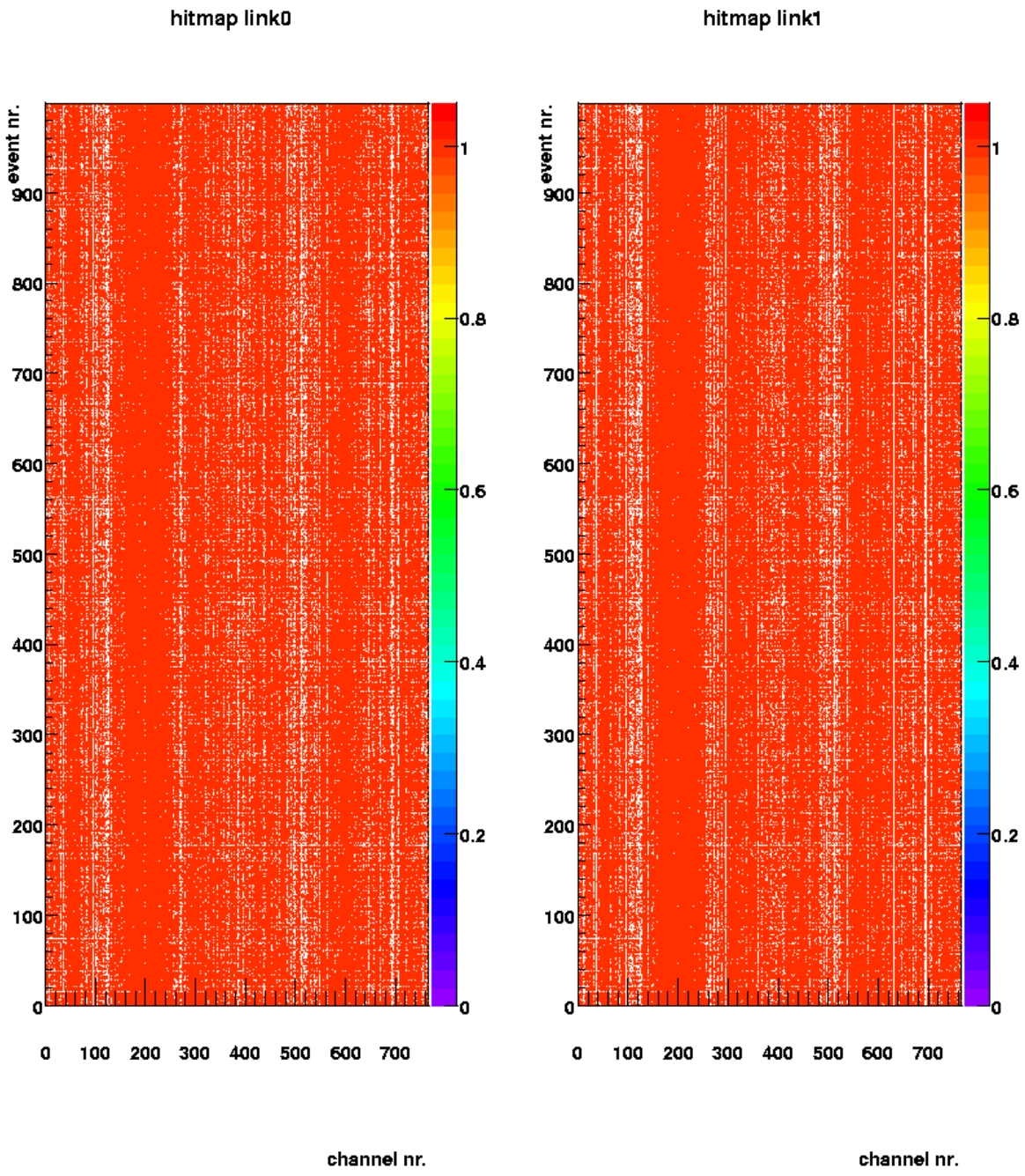

Figure 4.14: Hit map for both sides of k3112 without parasitic signal on cooling pipe

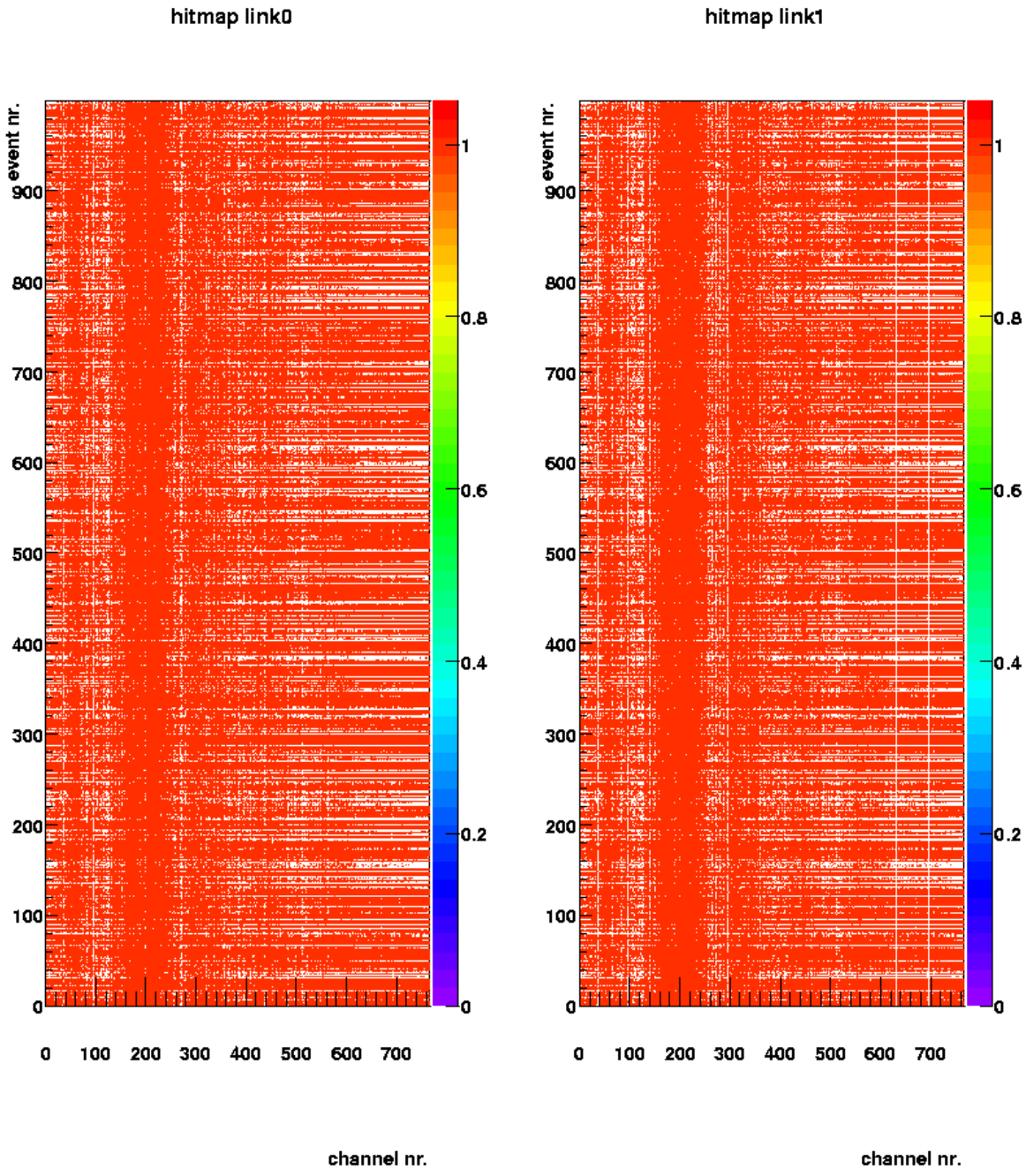

Figure 4.15: Hit map for k3112 with parasitic signal on cooling pipe

4.3.2 Injecting Noise on Power Tapes

Some work has been done on injecting noise on the power tapes of modules. A signal generator was used to inject different kinds of signals. Signals used were sinusoidal waves of different amplitudes and frequencies and random noise of different amplitudes and sampling frequencies. The greatest difficulty in doing these measurements was understanding what signal the module was receiving. An oscilloscope was used to measure the signal at different points of the system. Measurements were no good due to pickup from the air on the probes wires. The easiest place to inject signals is at PPB2. There was some fear that this would be too far from the module to actually affect them, as the power tapes act as very good noise filters. The measurements are of no interest if it is true that pickup on power tapes in ATLAS will be of lower frequencies than the ones which were injected. Two ways of injecting noise was tried. Noise was injected both with a differential signal between VCC and AGND at PPB2 and a common signal on VCC and AGND at PPB2.

The differential way of injecting a signal (fig. 4.16) was used in a test of scheme 1, to see the magnitude of effect that AC coupling at PPB1 between the grounds of VDD, VCC, HV and the sector shield has to the performance of the modules. It is a simple matter to remove and introduce the AC coupling at PPB1 with a set of jumpers. A signal was injected differentially between VCC and AGND at PPB2. The purpose of the test was to get some general knowledge of how pickup on power tapes affect modules with and without the AC coupling. Arranging a DC coupling between the lines and the shield was too difficult to implement at these sector positions at this stage. As both the proposed grounding schemes include some kind of coupling at PPB1, the results of this test would not be of any practical importance for choosing a scheme. The tests should be seen as an investigation of the effect this AC coupling has as it is one of the key elements in scheme 1.

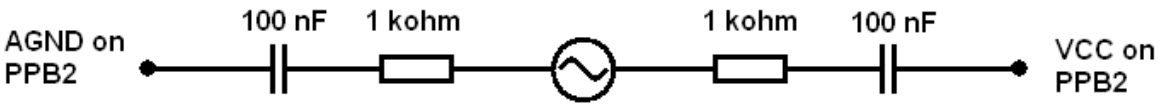

Figure 4.16: Injecting a differential signal with a signal generator at PPB2.

The voltage that I refer to as the signal amplitude is the amplitude set at the signal generator. The actual signal if any at the module could not be determined. The generator amplitude was slowly increased until excess noise was seen on the modules. Modules k3112, k3104 and scand1 on positions 3, 4 and 5 respectively were used in the test. All of them had shunt shields to the cooling pipe. Noise was injected on one module at a time. Measurements were made on all the modules but is presented only for the module to which noise was injected. Measurements were made both with and without chokes and compared to measurements without parasitic signal with chokes (tables 4.9, 4.10 and 4.11). All noise values are calculated with the stan_kwikgain macro.

Noise values seem to be a little bit higher with than without chokes. We seem to see a small reduction of noise on the bottom side of the modules when jumpers are inserted.

module	AC connection at PPB1	noise [mV] top	noise [mV] bottom	noise [e] top	noise [e] bottom	gain [mV/fC] top	gain [mV/fC] bottom
k3112	no	13.1	13.4	1321	1358	61.6	61.6
k3112	yes	13.1	13.3	1317	1354	61.7	61.7
ratio:		1.01	1.01	1.00	1.00	1.00	1.00
k3104	no	13.6	13.9	1575	1686	53.4	50.4
k3104	yes	13.6	13.8	1568	1676	52.9	50.1
ratio:		1.00	1.01	1.00	1.01 1.01	1.01	
scand1	no	12.9	12.6	1571	1501	53.7	53.7
scand1	yes	12.9	12.7	1575	1506	53.8	53.6
ratio:		1.00	0.99	1.00	1.00	1.00	1.00

Table 4.9: Module measurements without parasitic signal. General conditions: AC connection between module and cooling pipe, wrap from shield to PPB1, chokes inserted at PPB2.

module	AC connection at PPB1	noise [mV) top	noise [mV) bottom	noise [e] top	noise [e] bottom	gain [mV/fC] top	gain [mV/fC] bottom
k3112	no	13.4	14.9	1354	1469	61.5	61.5
k3112	yes	13.1	14.1	1326	1415	61.4	61.5
ratio:		1.02	1.06	1.02	1.04	1.00	1.00
k3104	no	13.7	14.6	1595	1766	53.2	50.2
k3104	yes	13.1	13.9	1572	1688	53.2	50.3
ratio:		1.05	1.05	1.01	1.05	1.00	1.00
scand1	no	15.1	13.6	1575	1610	53.5	53.4
scand1	yes	13.0	13.0	1573	1541	53.4	53.5
ratio:		1.01	1.05	1.00	1.04	1.00	1.00

Table 4.10: Module measurements without parasitic signal and with chokes removed. General conditions: AC connection between module and cooling pipe, wrap from shield to PPB1, no chokes.

module	AC at PPB1	signal	ampl. [V]	freq. [MHz]	noise [mV] top	noise [mV] bottom	noise [e] top	noise [e] bottom	gain [mV/fC] top	gain [mV/fC] bottom
scand1	no	sine	1	16	13.1	13.6	1567	1626	53.6	53.3
scand1	yes	sine	1	16	13.8	13.0	1605	1567	53.3	53.6
k3104	no	sine	1	4	14.3	15.3	1648	1826	53.5	50.3
k3104	yes	sine	1	4	13.5	13.7	1548	1675	53.5	50.4
k3104	no	sine	1	8	14.0	14.9	1607	1799	53.0	50.3
k3104	yes	sine	1	8	13.8	13.9	1602	1686	53.2	50.3
k3104	no	sine	1	16	14.1	15.1	1633	1844	53.2	50.3
k3104	yes	sine	1	16	13.7	14.2	1584	1725	53.0	50.1
k3104	no	sine	1	32	13.7	14,5	1580	1747	53.3	50.3
k3104	yes	sine	1	32	13.4	13.7	1541	1665	53.6	50.5
k3104	no	random	1	4	13.8	14.8	1605	1797	53.4	50.2
k3104	yes	random	1	4	13.5	13.8	1555	1678	53.5	50.5
k3104	no	random	1	8	13.9	14.8	1612	1801	53.4	50.4
k3104	yes	random	1	8	13.5	13.8	1553	1676	53.4	50.5
k3104	no	random	1	16	13.9	14.8	1621	1794	53.1	50.2
k3104	yes	random	1	16	13.3	13.9	1567	1682	53.5	50.6
k3104	no	random	1	32	14.0	14.8	1631	1816	53.4	50.4
k3104	yes	random	1	32	13.8	13.9	1596	1694	52.9	50.2

Table 4.11: Module measurements with differential parasitic signal. General conditions: AC connection between module and cooling pipe, wrap from shield to PPB1, chokes inserted at PPB2.

A test was done injecting a common signal on VCC and AGND (fig. 4.17) as there are reasons for believing that this is the kind of pickup we can expect on power tapes. Conclusions we can draw from these measurements are that the bottom side chips are more affected than the top side chips and the edge chips are more affected than the inner chips (table 4.12, fig. 4.18 and 4.19).

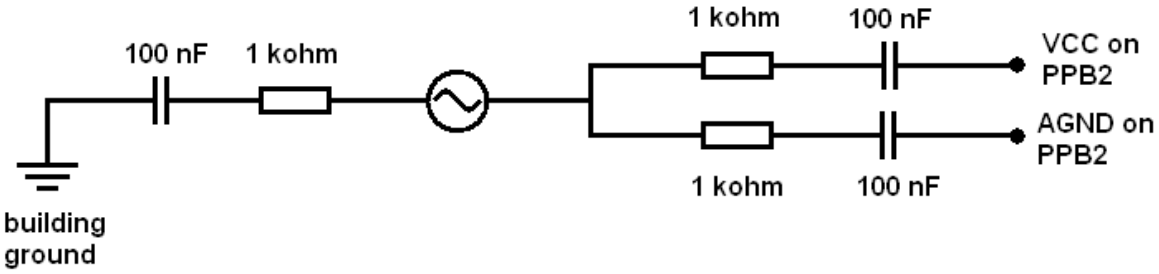

Figure 4.17: Injecting a common signal with a signal generator at PPB2.

module	AC at PPB1	signal	ampl. [V]	freq. [MHz]	noise [mV] top	noise [mV] bottom	noise [e] top	noise [e] bottom	gain [mV/fC] top	gain [mV/fC] bottom
k3104	no	sine	1.5	8	14.1	14.5	1634	1716	53.3	50.2
k3104	yes	sine	1.5	8	14.4	14.7	1655	1756	53.5	50.6
k3104	no	sine	2	8	19.8	21.2	2334	2298	53.5	50.8
k3104	yes	sine	2	8	20.4	21.7	2359	2650	53.2	50.7
k3104	no	sine	3	8	25.1	27.2	3014	3422	53.2	50.5
k3104	yes	sine	3	8	25.9	28.1	3092	3191	53.1	50.8
scand1	no	sine	1.5	8	12.7	15.8	1679	1733	53.6	53.5
scand1	yes	sine	1.5	8	13.1	13.3	1566	1574	53.9	53.8
scand1	no	sine	2	8	15.3	17.0	1736	1868	53.7	53.3
scand1	yes	sine	2	8	13.1	13.4	1568	1584	53.4	53.3
scand1	no	sine	3	8	16.3	20.0	1914	2251	53.4	52.9
scand1	yes	sine	3	8	14.8	13.8	1647	1657	53.8	53.5
k3112	no	sine	1.5	8	13.4	15.3	1346	1495	61.4	61.5
k3112	yes	sine	1.5	8	13.3	15.6	1348	1456	61.2	61.3
k3112	no	sine	2	8	15.4	25.9	1551	2597	61.6	61.2
k3112	yes	sine	2	8	15.5	25.2	1559	2591	61.2	61.2
k3112	no	sine	3	8	17.4	33.6	1795	3386	61.1	61.1
k3112	yes	sine	3	8	17.3	36.5	1789	3298	61.3	61.4

Table 4.12: Module measurements with common parasitic signal. General conditions: AC connection between module and cooling pipe, wrap from shield to PPB1, chokes inserted at PPB2.

4.4 Conclusions

A great increase in noise of placing modules in system conditions was not seen. This is good news although it makes the task of choosing grounding and shielding scheme difficult. Several different module configurations have been tested and most test give similar performance values for each module. The measurements that give an increase in noise are the ones where chokes are removed from the system and the ones where an artificial signal is applied to the system. More modules have to be put in a system. As of December 2000 modules had only been read out from one cooling pipe. The effect of radial overlap had not been tried. There is room for improvement of the implementation of the grounding schemes if excess noise is seen in the future. As of the test of scheme 1, we have not tried having adjacent modules with power cabling routed out of the test sector in different directions. Trying this while injecting noise in the big ground loop which is created would be interesting. The most interesting results so far from the noise injection measurements are the chip and side dependance. Improved understanding of noise injection would probably contribute to understanding what grounding scheme should be chosen.

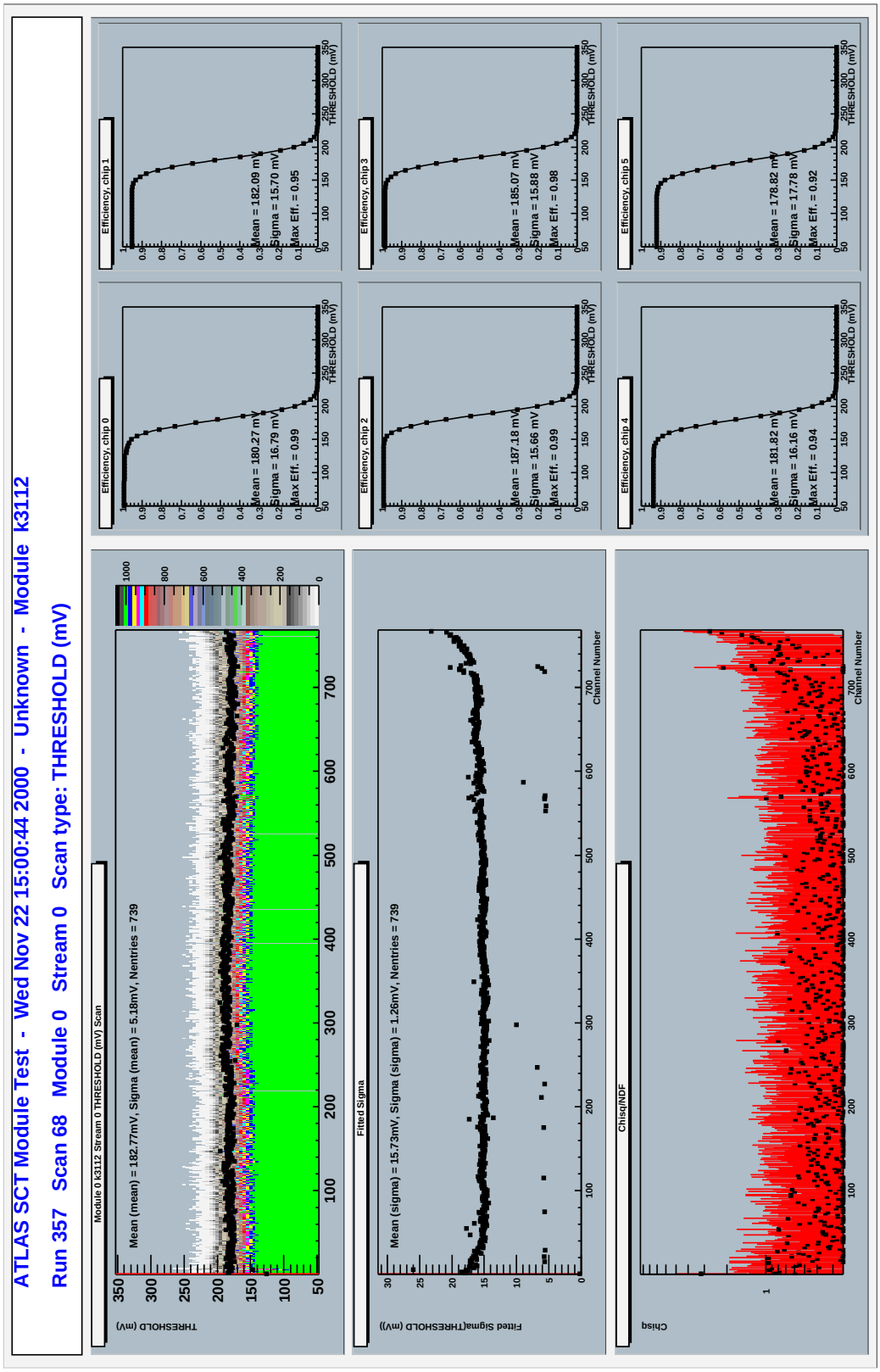

Figure 4.18: Threshold scan of top side of k3112 with 2 fC calibration charge and a common parasitic signal injected on power tapes (2 V, 8 MHz, sinusoidal signal)

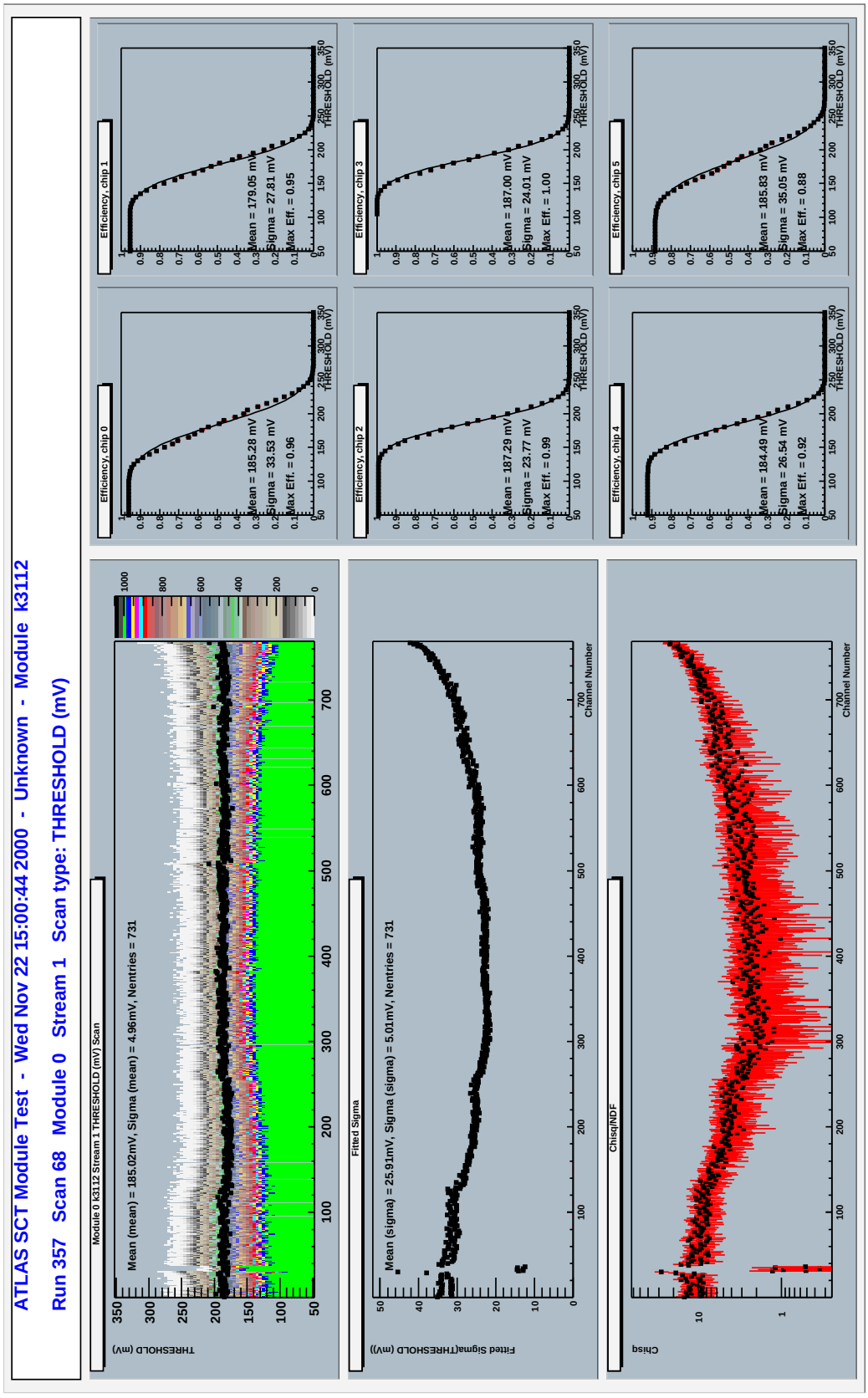

Figure 4.19: Threshold scan of bottom side of k3112 with a 2 fC calibration charge and a common parasitic signal injected on power tapes (2 V, 8 MHz, sinusoidal signal)

Bibliography

[1] Allport P., *ATLAS silicon strip detector new spec*, 1996
http://atlas.kek.jp/managers/silicon/si_det/newspec.ps

[2] ATLAS Collaboration, *ATLAS Web Page*
http://greybook.cern.ch/

[3] ATLAS Inner Detector Community, *ABCD3T ASIC Project Specification Version V1.1*, 2000
http://scipp.ucsc.edu/groups/atlas/elect-doc/ABCD3T_Spec_v1.1.pdf

[4] ATLAS Inner Detector Community, *ATLAS98-99 layout*, 1999
http://atlas.kek.jp/managers/silicon/si_det/Abnormalcurrentfix.doc.pdf

[5] ATLAS Inner Detector Community, *Inner Detector TDR*, 1997
ATLAS TDR 5, CERN/LHCC 97-17

[6] Baines J., *ATLAS SCT Picture Library*
http://hepunx.rl.ac.uk/atlasuk/sct/pictlib/

[7] Brückman de Renstrom P., *Talk in the December SCT week*, 2000
http://atlas.web.cern.ch/Atlas/GROUPS/INNER_DETECTOR/SCT/systemtest/PBDec00/

[8] Cindro V., *Power Tape Web Page*
http://www-f9.ijs.si/atlas/welcome.html

[9] Feld L., *How to Evaluate Common Mode Noise in a Digital Read Out System*, 2000
http://runt1.physik.uni-freiburg.de/feld/sct/common_mode

[10] Gadomski S. Pater J. etc., *System Test Web Page*
http://atlas.web.cern.ch/Atlas/GROUPS/INNER_DETECTOR/SCT/systemtest/

[11] Moorhead G., *ATLAS SCT Module/Hybrid Test DAQ*
http://atlas.web.cern.ch/Atlas/GROUPS/INNER_DETECTOR/SCT/testdaq/testdaq.html

[12] Peeters S., *SCTDAQ and Common Mode Noise*, 2000
http://www.nikhef.nl/∼r92/systemtest/common_mode/

[13] Roe S., *Motivation for Analogue Readout in the ATLAS SCT*, 1998
http://sroe.home.cern.ch/sroe/Motivation.html

[14] Smith T., *Transparencies from Feb 00 grounding and shielding meeting*, 2000
http://hep.ph.liv.ac.uk:80/∼smithy/atlas/gndshld/gndshld.htm

[15] Spencer N., *ATLAS SCT/Pixel Grounding Shielding Note*, 1999
http://scipp.ucsc.edu/groups/atlas/elect-doc/SCT_GND_SHIELD2.pdf

[16] Szoncsó F., *Supplying High-Energy Physics Detector Systems*, 1996
http://s.home.cern.ch/s/szoncso/www/EMC/HEPDetSuppSys.html

[17] Unno Y. et al.,*Diagnosis of the abnormal leakage currents in the SCT Silicon microstrip detetors*
http://atlas.kek.jp/managers/silicon/si_det/ATLAS98/ATLAS98d991223.pdf

List of Figures

List of Tables